Exploring the impacts of unprecedented climate extremes on forest ecosystems: hypotheses to guide modeling and experimental studies

Jennifer A. Holm[1,*], David M. Medvigy[2], Benjamin Smith[3,4], Jeffrey S. Dukes[5], Claus Beier[6], Mikhail Mishurov[3], Xiangtao Xu[7], Jeremy W. Lichstein[8], Craig D. Allen[9], Klaus S. Larsen[6], Yiqi Luo[10], Cari Ficken[11], William T. Pockman[12], William R.L. Anderegg[13], and Anja Rammig[14]

[1] Lawrence Berkeley National Laboratory, Berkeley, California, USA
[2] University of Notre Dame, Notre Dame, Indiana, USA
[3] Dept of Physical Geography and Ecosystem Science, Lund University, Lund, Sweden
[4] Hawkesbury Institute for the Environment, Western Sydney University, Penrith, NSW 2751, Australia
[5] Department of Forestry and Natural Resources and Biological Sciences, Purdue University, West Lafayette, Indiana, USA
[6] Department of Geosciences and Natural Resource Management, University of Copenhagen, Frederiksberg, Denmark
[7] Department of Ecology and Evolutionary Biology, Cornell University, Ithaca, New York, USA
[8] Department of Biology, University of Florida, Gainesville, Florida, USA
[9] U.S. Geological Survey, Fort Collins Science Center, New Mexico Landscapes Field Station, Los Alamos, New Mexico, USA
[10] Center for Ecosystem Science and Society, Department of Biological Sciences, Northern Arizona University, Flagstaff, Arizona, USA
[11] Department of Biology, University of Waterloo, Waterloo, Ontario, Canada
[12] Department of Biology, University of New Mexico, Albuquerque, New Mexico, USA
[13] School of Biological Sciences, University of Utah, Salt Lake City, Utah, USA
[14] Technical University of Munich, TUM School of Life Sciences Weihenstephan, Freising, Germany

* *Correspondence to*: Jennifer Holm; 510-495-8083; jaholm@lbl.gov

Keywords: demographic modeling; mortality; drought; recovery; carbon cycle; nonstructural carbohydrate storage; plant hydraulics; dynamic vegetation

Abstract

Climatic extreme events are expected to occur more frequently in the future, increasing the likelihood of unprecedented climate extremes (UCEs), or record-breaking events. UCEs, such as extreme heatwaves and droughts, substantially affect ecosystem stability and carbon cycling by increasing plant mortality and delaying ecosystem recovery. Quantitative knowledge of such effects is limited due to the paucity of experiments focusing on extreme climatic events beyond the range of historical experience. Here, we present a road map of how two dynamic vegetation demographic models (VDMs) can be used to investigate hypotheses surrounding ecosystem responses to UCEs (e.g., unprecedented droughts). As an example, we investigate whether ecosystem responses to UCEs are qualitatively different from responses to milder extremes, as a result of non-linear ecosystem responses. Additionally, we explore how unprecedented droughts in combination with increasing atmospheric CO_2 and/or temperature may affect ecosystem stability and carbon cycling. We explored these questions using simulations of pre-drought and post-drought conditions at well-studied forest sites in Australia and Costa Rica, using the ED2 and LPJ-GUESS models. Both models produced nonlinear responses to UCEs. Due to the two models having different but plausible representations of processes and interactions, they diverge in sensitivity of biomass loss due to drought duration or intensity, and differ between each site. Biomass losses are most sensitive to drought duration in ED2, but to drought intensity in LPJ-GUESS. Elevated atmospheric CO_2 concentrations (eCO_2) alone did not completely buffer the ecosystems from carbon losses during UCEs in the majority of our simulations. Our findings highlight contrasting differences in process formulations and uncertainties in models, notably related to availability in plant carbohydrate storage and the diversity of plant hydraulic schemes, in projecting potential ecosystem responses to UCEs. Our model review uncovered different underlying hypotheses of plant responses to UCEs, reflecting knowledge gaps, which should be tested with targeted field experiments and an iterative modeling-experimental conceptual framework.

1 Introduction

The increase in extreme climate and weather events, such as prolonged heatwaves and droughts as seen over the last three decades, are expected to continue to increase in frequency and magnitude, leading to progressively longer and warmer droughts on land (IPCC 2012, 2021). Droughts are affecting all areas of the globe, more than any other natural disturbance, and recent droughts have broken long-standing records (Ciais et al., 2005; Phillips et al., 2009; Williams et al., 2012; Matusick et al., 2013; Griffin and Anchukaitis, 2014; Asner et al., 2016; Feldpausch et al., 2016; Seneviratne et al., 2021). Such 'unprecedented climate extremes' (UCEs; "record-breaking events", IPCC (2012)) that are larger in extent and longer-lasting than historical norms can have dramatic consequences for terrestrial ecosystem processes, including carbon uptake and storage and other ecosystem services (Reichstein et al., 2013; Settele, 2014; Allen et al., 2015; Brando et al., 2019; Kannenberg et al., 2020). Thus, to better anticipate the implications of climatic changes for the terrestrial carbon sink and other ecosystem services, we need to better understand how ecosystems respond to extreme droughts and other UCEs.

To learn how ecosystems respond to rarely experienced or unprecedented conditions, ecologists can experimentally manipulate environmental conditions (Rustad, 2008; Beier et al., 2012; Meir et al., 2015; Aguirre et al., 2021). However, the majority of such experiments apply moderate treatments, which are mostly weaker in intensity and/or shorter in duration than potential future UCEs (Beier et al., 2012; Kayler et al., 2015; but see Luo et al., 2017), and single experiments have low power to detect effects of stressors on ecosystem responses (Yang et al., 2022). Additionally, most experiments examine low-stature ecosystems, such as grassland, shrubland or tundra, due to lower requirements for infrastructure and financial investment compared to mature forests. However, forests may respond qualitatively differently to UCEs than other ecosystems, in part due to mortality of large trees and strong nonlinear ecosystem responses, with long-lasting consequences for ecosystem-climate feedbacks (Williams et al., 2014; Meir et al., 2015). Ecosystem responses to naturally occurring extreme droughts and heatwaves have been documented (Ciais et al., 2005; Breshears et al., 2009; Feldpausch et al., 2016; Matusick et al., 2016; Ruthrof et al., 2018; Powers et al,. 2020); however, these rapidly-mobilized post-hoc studies often are unable to measure all critical variables and may lack consistently collected data for comparison with pre-drought conditions, thus limiting their inferential power and ability to improve quantitative models. The difficulties of performing

controlled real-world experiments of UCEs at broad spatial and temporal scales make process-based modeling a valuable tool for studying potential ecosystem responses to extreme events.

Process-based models can be used to explore potential ecosystem impacts using projected climate change over broad spatial and temporal scales (Gerten et al., 2008; Luo et al., 2008; Zscheischler et al., 2014; Sippel et al., 2016), as seen in a few modeling studies that have synthesized and improved our process-level understanding of UCE effects (McDowell et al., 2013; Dietze and Matthes, 2014). However, due to the overly simplified representation of ecological processes in most land surface models (LSMs) – the terrestrial components of Earth System Models (ESMs) used for climate projections – it is doubtful whether most of these models adequately capture ecosystem feedbacks and other responses to UCEs (Fisher and Koven, 2020). For example, only a few ESMs in recent coupled model intercomparison projects (CMIP6) and IPCC climate assessments (Ciais et al., 2013; Arora et al., 2020) include vegetation demographics (Döscher et al., 2022), and most rely on prescribed, static maps of plant functional types (PFTs) (Ahlström et al., 2012). Other LSMs simulate PFT shifts (i.e., dynamic global vegetation models, DGVMs; Sitch et al., (2008)) based on bioclimatic limits, instead of emerging from the physiology- and competition-based demographic rates that determine resource competition and plant distributions in real ecosystems (Fisher et al., 2018). Although a new generation of LSMs with more explicit ecological dynamics and structured demography is emerging (Holm et al., 2020; Koven et al., 2020; Döscher et al., 2022), most current ESMs are limited in ecological detail and realism (e.g., ecosystem structure, demography, and disturbances). Failing to mechanistically represent mortality, recruitment, and disturbance – each of which influences biomass turnover and carbon (C) allocation (Friend et al., 2014) – limits the ability of these models to realistically forecast ecosystem responses to anomalous environmental conditions like UCEs (Fisher et al., 2018).

Evaluating and improving the representation of physiological and ecological processes in ecosystem models is critical for reducing model uncertainties when projecting the effects of UCEs on long-term ecosystem dynamics and functioning (Table 1). Vegetation demography, plant hydraulics, enhanced representations of plant trait variation, explicit treatments of resource competition (e.g., height-structured competition for light), and representing major disturbances (e.g., extreme drought) have all been identified as critical areas for advancing current models (Scheiter et al., 2013; Fisher et al., 2015; Weng et al., 2015; Choat et al., 2018; Fisher et al.,

2018; Blyth et al., 2021) and are necessary advances for realistically representing the ecosystem impacts of UCEs. In this perspectives focused paper we look at the differences in these processes, and how they contribute to uncertainty across multiple temporal phases surrounding an extreme event: predicting an ecosystem's pre-drought resistance, which influences the degree of impact and recovery from UCEs (Table 1) (ca. Frank et al., 2015).

In order to inform our discussion, we explore the potential responses of forest ecosystems to UCEs using two state-of-the-art process-based demographic models (vegetation demographic models, VDMs; Fisher et al., (2018)), a unique model exploration-discussion approach to help highlight new paths forward for model advancement. We first present conceptual frameworks and hypotheses on potential ecosystem responses to UCEs based on current knowledge. We then present VDM simulations for a range of hypothetical UCE scenarios to illustrate current state-of-the-art model representations of eco-physiological mechanisms expected to drive responses to UCEs. While a variety of UCE-linked biophysical tree disturbance processes (e.g., fire, wind, insect outbreaks) can drive non-linear ecosystem responses, we focus specifically on extreme droughts, which have important impacts on many ecosystems around the world (e.g. Frank et al., 2015, IPCC 2021). By studying modeled responses to UCEs, we explore the limits to our current understanding of ecosystem responses to extreme droughts and their corresponding thresholds and tipping points. As anthropogenic forcing has increased the frequency, duration, and intensity of droughts throughout the world (Chiang et al., 2021), we explore how eCO_2 and rising temperatures may affect drought-induced C loss and recovery trajectories, and how the scientific community can iteratively address these questions through experiments and modeling studies. We believe the combination of using cutting-edge VDMs alongside a review of current gaps in knowledge will help guide modeling and experimental advances in order to address novel forest responses to climate extremes.

1.1 Conceptual and Modeling Framework for Hypothesis Testing:

We combine conceptual frameworks (Fig. 1) and ecosystem modeling to test two hypotheses on potential responses of plant carbon stocks to UCEs. The first hypothesis is: ***Hypothesis (H1). Terrestrial ecosystem responses to UCEs will differ qualitatively from ecosystem responses to milder extremes because responses are nonlinear. Nonlinearities can***

153 ***arise from multiple mechanisms – including shifts in plant hydraulics, C allocation,***
154 ***phenology, and stand demography – and can vary depending on the pre-drought state of the***
155 ***ecosystem.***

156 We present four conceptual relationships that describe terrestrial ecosystem responses to varying
157 degrees of extreme events (Fig. 1). Change in vegetation C stock is *linearly* related to drought
158 intensity and/or drought duration (Fig. 1a, H0, null hypothesis), which has some observational
159 support from annual and perennial grassland ecosystems, shrublands and savannas across the
160 globe (Bai et al., 2008; Muldavin et al., 2008; Ruppert et al., 2015). Alternatives to the null
161 (linear) hypothesis are that biomass loss increases non-linearly with increased drought intensity
162 (i.e., reduction in precipitation) represented by a threshold-based relationship (Fig. 1a, H1a),
163 increased drought duration (i.e., prolonged drought with the same intensity) by shifting the linear
164 relationship downwards via increasing slopes (Fig. 1a, H1b), or the combination of both intensity
165 and duration (Fig. 1a, H1c). These hypotheses are supported by observations from the Amazon
166 Basin and Borneo (Phillips et al., 2010) where tree mortality rates increased non-linearly with
167 drought intensity. Similarly, plant hydraulic theories predict nonlinear damage to the plant-water
168 transport systems, and thus mortality risk, as a function of drought stress (Sperry and Love,
169 2015). In particular, longer droughts are more likely to lead to lower soil water potentials,
170 leading to a nonlinear xylem damage function even if stomata effectively limit water loss (Sperry
171 et al., 2016).

172 ***Hypothesis (H2): The effects of increasing atmospheric CO_2 concentration (eCO_2) will***
173 ***alleviate impacts of extreme drought stress through an increase in vegetation productivity and***
174 ***water-use efficiency, but only up to a threshold of drought severity, while increased***
175 ***temperature (and related water stress) will exacerbate tree mortality.***

176 This second hypothesis is based on growing evidence that effects of eCO_2 and climate
177 warming may interact with effects of drought intensity on ecosystems. The CO_2 fertilization
178 effect enhances vegetation productivity (e.g., net primary production, NPP) (Ainsworth and
179 Long, 2005; Norby et al., 2005; Wang et al., 2012), but this fertilization effect is generally
180 reduced by drought (Hovenden et al., 2014; Reich et al., 2014; Gray et al., 2016). Drought events
181 often coincide with increased temperature, which intensifies the impact of drought on
182 ecosystems (Allen et al., 2015; Liu et al., 2017), resulting in nonlinear responses in mortality

183 rates (Adams et al., 2009; Adams et al., 2017a). The evaluation of C cycling in VDMs with
184 doubling of CO_2 (only "beta effect") showed a large carbon sink in a tropical forest (Holm et al.,
185 2020), but the inclusion of climate interactions in VDMs needs to be further explored.

186 Here, we relate ecosystem responses to UCEs by calculating the "integrated carbon (C)
187 loss" (Fig. 1b and see Methods), which integrates C loss from the beginning of the drought until
188 the time when C stocks have recovered to 50% of the pre-drought level. In response to drought,
189 warming, and eCO_2, divergent potential C responses (gains and losses; Fig. 1c) can be expected
190 (Keenan et al., 2013; Zhu et al., 2016; Adams et al., 2017a). For example, a grassland
191 macrocosm experiment found that eCO_2 completely compensated for the negative impact of
192 extreme drought on net carbon uptake due to increased root growth and plant nitrogen uptake,
193 and led to enhanced post-drought recovery (Roy et al., 2016). However, a 16-year grassland
194 FACE and the SoyFACE experiments showed that CO_2 fertilization effects were reduced or
195 eliminated under hotter/drier conditions (Gray et al., 2016; Obermeier et al., 2016). Reich et al.,
196 (2014) also found that CO_2 fertilization effects were reduced in a perennial grassland by water
197 and nitrogen limitation.

198 A corollary to our H2 is that conditions that favor productivity (e.g., longer growing
199 seasons and/or CO_2 fertilization) will enhance vegetation growth leading to "structural
200 overshoot" (SO; Fig. 1d; adapted from and supported by Jump et al., 2017), and can amplify the
201 effects of UCEs. Enhanced vegetation growth coupled with environmental variability can lead to
202 exceptionally high plant-water-demand during extreme drought and water stress, resulting in a
203 "mortality overshoot" (MO; Fig 1d). We conceptualize how oscillations between SO and
204 associated MO could be amplified by increasing climatic variability and UCEs (Fig. 1d).
205 Confidence is low as to how historically unprecedented eCO_2 levels and temperatures will affect
206 ecosystems in the future (i.e., the widening of the shaded areas compared to historical, Fig. 1d).
207 We expect, however that a rapidly changing climate, combined with effects of UCEs as a result
208 of more frequent extreme drought/heat events and drought stress, can exacerbate and amplify
209 SOs and MOs (Jump et al., 2017), leading to increasing C loss, even though various buffering
210 mechanisms exist (cf. (Lloret et al., 2012; Allen et al., 2015)). Relative to our conceptual (Fig.
211 1d), we note that most experimental, observational and modeling studies (Ciais et al., 2005; da
212 Costa et al., 2010; Phillips et al., 2010; Meir et al., 2015) take into account only low to moderate

drought intensities or single events, or combine drought with moderate effects of temperature change. As represented by the increasing amplitude of oscillations in Fig. 1d, the interactions between increased temperatures, UCE events, and vegetation feedbacks make ecosystem states become inherently unpredictable, particularly over longer time-scales.

2 Methods

We explored our hypotheses at forested ecosystems in Australia and Central America using two VDMs: the Lund-Potsdam-Jena General Ecosystem Simulator (LPJ-GUESS) (Smith et al., 2001; Smith et al., 2014) and the Ecosystem Demography model 2 (ED2) (Medvigy et al., 2009; Medvigy and Moorcroft, 2012). These models include detailed process representation of ecosystem demography and dynamic plant growth, recruitment, and mortality, resulting in changes in abundance of different PFTs, as well as vertically stratified tree size- and age-class structure. Community dynamics and age-/size-structure are emergent properties from competition for light, space, water, and nutrients, which dynamically and explicitly scale up from the tree, to stand, to ecosystem level.

VDMs have been used to interpret the cascade of ecosystem responses to long-term droughts in the Amazon and are informative when conducting model-data comparisons (Powell et al., 2013), but studies of ecosystem responses to UCEs are lacking. New implementation of plant competition for resources and plant hydraulics in VDMs are improving our understanding of plant-water relations and stresses within plants (Christoffersen et al., 2016; Xu et al., 2016; Fisher et al., 2018; and see Kennedy et al., 2019 for representation in a 'big-leaf' model). Since field data needed to evaluate UCE responses are, by definition, unavailable, we do not perform model-data comparisons. Rather, we use the model results and conceptual framework as a road map to explore our hypotheses and illustrate their implications for ecosystem responses under UCEs, not historical drought events.

2.1 LPJ-GUESS and ED2 Model Descriptions

Both LPJ-GUESS and ED2 resolve vegetation into tree cohorts characterized by their PFT, in addition to age-class in LPJ-GUESS; and size, and stem number density in ED2. Both models are driven by external environmental drivers (e.g., temperature, precipitation, solar radiation, atmospheric CO_2 concentration, nitrogen deposition), and soil properties (soil texture,

depth, etc.), and also depend on dynamic ecosystem state, which includes light attenuation, soil moisture, and soil nutrient availability. Establishment and growth of PFTs, and their carbon-, nitrogen- and water-cycles, are simulated across multiple patches per grid cell to account for landscape heterogeneity. Both models characterize PFTs by physiological and bioclimatic parameters, which vary between the models (Smith et al., 2001; Smith et al., 2014; Medvigy et al., 2009; Medvigy and Moorcroft, 2012).

The LPJ-GUESS includes three woody PFTs: evergreen, intermediate evergreen, and deciduous PFTs. Mortality in LPJ-GUESS is governed by a 'growth-efficiency'-based function (kg C m^{-2} leaf yr^{-1}), which captures effects of water deficit, shading, heat stress, and tree size on plant productivity relative to its resource-uptake capacity (leaf area), with a threshold below which stress-related mortality risk increases markedly, in addition to background senescence and exogenous disturbances. Stress mortality can be reduced by plants using labile carbon storage, modeled implicitly using a 'C debt' approach, which buffers low productivity, enhancing resilience to milder extremes (more details are given in section 4.1.4). Total mortality can thus be impacted by variation in environmental conditions such as water limitation, low light conditions, and nutrient constraints, as well as current stand structure (Smith et al., 2001; Hickler et al., 2004).

The ED2 version used here (Xu et al., 2016) includes four woody PFTs: evergreen, intermediate evergreen, deciduous, brevi-deciduous, and deciduous stem-succulent. This ED2 version includes coupled photosynthesis, plant hydraulics, and soil hydraulic modules (Xu et al., 2016), which together determine plant water stress. The plant hydraulics module tracks water flow along a soil–plant–atmosphere continuum, connecting leaf water potential, stem sap flow, and transpiration, thus influencing controls on photosynthetic capacity, stomatal closure, phenology, and mortality. Leaf water potential depends on time-varying environmental conditions as well as time-invariant PFT traits. Leaf shedding is triggered when leaf water potential falls below the turgor loss point (a PFT trait) for a sufficient amount of time. Leaf flushing occurs when stem water potential remains high (above half of the turgor loss point) for a sufficient time (see Xu et al., 2016 for details). PFTs differ in their hydraulic traits, wood density, specific leaf area, allometries, rooting depth, and other traits. Stress-based mortality in the ED2 version used here includes two main physiological pathways in our current

understanding of drought mortality (McDowell et al., 2013): C starvation and hydraulic failure. Mortality due to C starvation in ED2 results from a reduction of C storage, a proxy for non-structural carbohydrate (NSC) storage, which integrates the balance of photosynthetic gain and maintenance cost under different levels of light and moisture availability. Mortality due to hydraulic failure in ED2 is based on the percentage loss of stem conductivity. ED2 also includes a density-independent senescence mortality rate based on wood density.

2.2 Modeling protocol

To exemplify how VDMs can be tools to explore new hypotheses related to UCEs we applied the models at two field sites, that were chosen due to being extensively studied and the models used here have already been run at these sites and previously benchmarked against field data (see Xu et al., 2016; Medlyn et al., 2016; Medvigy et al., 2019 for model-data validation). The purpose of this paper was not to do a large multi-site comparison, but rather just select a few for hypothesis testing. In addition, the two sites span a range of vegetation types and are in warm, seasonally dry climates that are more likely to experience droughts in the future (Allen et al., 2017). The first is a mature *Eucalyptus* (*E. tereticornis*) warm temperate-subtropical transitional forest that is the site of the Eucalyptus Free Air CO_2 enrichment (EucFACE) experiment in Western Sydney, Australia (Medlyn et al., 2016; Ellsworth et al., 2017; Jiang et al., 2020), with a canopy coverage of 95% (830 trees ha^{-1}). The EucFACE site has a mean annual temperature of 17.3°C, receives an annual rainfall of 800 mm (Ellsworth et al., 2017), with total plant available soil water of 300 mm. The evergreen eucalypt trees are on average 22 m tall with a DBH of 21 cm and a stand-level LAI of 1.7 m^2 m^{-2}. The second site is a seasonally dry tropical forest in the Parque Nacional Palo Verde in Costa Rica (Powers et al., 2009). This site has nutrient rich soils (Powers and Peréz-Aviles, 2013), stand basal area is 29.2 (± 8.1) m^2 ha, stem density of 64 (± 12) trees ha^{-1}, and a mean annual temperature of 25.1°C, and mean annual rainfall of 1440 mm, with a 5-month dry season. Multiple leaf phenological strategies co-occur, including evergreens, brevi-deciduous tree species, as well as deciduous species that drop their leaves during the dry season, leading to a strong seasonality in LAI ranging from 3 to 4.5, but can get as low as 1.2 m^2 m^{-2} (Kalacska et al., 2005).

We performed a 100-year "baseline" simulation for each model at each site driven by constant, near ambient, atmospheric CO_2 (400 ppm) and recycled historical site-specific climate

data (1992-2011 for EucFACE and 1970-2012 for Palo Verde; Sheffield et al., (2006)), absent of drought treatments. A detailed description of the meteorological data and initial conditions used to drive the models is in the Supplementary Text A. The two models were previously tuned for each site (Xu et al., 2016; Medlyn et al., 2016), and no additional site-level parameter tuning was conducted here due to evaluating responses from hypothetical UCEs. To describe the ecosystem impact of UCEs, we simulated 10 years of pre-drought conditions (continuing from the baseline simulation), followed by drought treatments that differed in intensity and duration, followed by a 100-year post-drought recovery period. To explore the effects of drought intensity, we conducted 20 different artificial drought intensity simulations, in which precipitation during the whole year is reduced by 5% to 100% of its original amount, in increments of 5%. To explore the effects of drought duration, the 20 different drought intensities are maintained over 1, 2 and 4 years (Table S1). We examined model responses of aboveground biomass, leaf area index (LAI), stem density (number ha^{-1}), plant available soil water (mm), plant C storage (kg C m^{-2}), change in stem mortality rate (yr^{-1}), and PFT composition.

To explore how temperature, eCO_2 concentration, and UCE droughts influence forest C dynamics individually and in combination, we implemented the following five experimental scenarios, some realistic and others hypothetical, for each model (Table S1): increased temperature only (+2K over ambient), eCO_2 only (600 ppm and 800 ppm), and both increased temperature and eCO_2 (+2K 600 ppm; +2K 800 ppm). Temperature and eCO_2 manipulations were applied as step increases over the baseline conditions, and are artificial scenarios, as opposed to model-generated climate projections.

2.3 Linking concepts, hypotheses, and model outcomes

To relate our simulation results to Fig. 1a, we compared the total biomass loss as a result of each drought treatment by calculating the percentage of biomass reduction at the end of the drought period relative to the baseline (no drought) simulation. To explicitly consider biomass recovery rates over time, we calculated "integrated-C-loss" (Eqs. 1-3), as a result of drought under current climate, which are determined based on the concepts in Fig. 1b. We defined "integrated-C-loss" as the time-integrated carbon in biomass that is lost due to drought relative to what the vegetation would have stored in the absence of drought. That is, it is the difference between biomass in the presence of drought (B_d) at time (t) and biomass in the baseline

simulation (no drought; B_{base}), integrated over a defined recovery time period (in kg C m^{-2} yr):

$$\text{Integrated-C-loss} = \int_{t=t_1}^{t=t_2} (B_{base}(t) - B_d(t))\, dt \quad \text{(Eq. 1)}$$

To define the bounds of integration, in Eq. 1, t_1 is defined as the time when the maximum amount of plant C is lost as a result of the drought:

$$B_{base}(t_1) - B_d(t_1) = \max_t [B_{base}(t) - B_d(t)] \quad \text{(Eq. 2)}$$

Then, t_2 is defined implicitly as the time when 50% of the lost biomass has been recovered compared to the baseline:

$$B_{base}(t_2) - B_d(t_2) = \frac{1}{2}(B_{base}(t_1) - B_d(t_1)) \quad \text{(Eq. 3)}$$

Since all integrated-C-loss results are taken as the difference from a non-drought baseline biomass (B_{base}) and all droughts will result in a loss of C.

We also use integrated-C-loss to examine the role of drought, temperature and eCO_2 change for moderating or exacerbating the impacts of drought on forest C stocks; i.e., to evaluate the hypotheses illustrated in Fig. 1c. To assess these impacts of changing climates, we calculate an "integrated-C-change" (Eq. 4). Defined as the difference between the integrated-C-loss due to drought alone (Eqs. 1-3) under present climate, and the integrated-C-loss due to the combined effects of drought and climate change (i.e., five scenarios of temperature increase and eCO_2):

$$\text{Integrated-C-change} = integrated\ C\ Loss_{Drought} - integrated\ C\ Loss_{Drought+CC} \quad \text{(Eq. 4)}$$

Because we expect drought to reduce vegetation C stocks, and thus integrated-C-loss to be negative, positive values of integrated-C-change indicate that changes in climatic drivers reduced the C losses from drought (i.e., buffering effects). Negative values of integrated-C-change indicate that the climate change scenario leads to either greater C losses or losses that persist for longer amounts of time (i.e., magnitude and/or duration) compared to a simulation with no climate change (i.e., "reference" run).

3 Results

As a basis for the treatment results presented here, we compared the baseline simulations (prior to drought or climate change treatments) of the two VDMs to observations at both sites for biomass and LAI (Table S2, Fig. S1). Both models had similar biomass compared to observations at Palo Verde (10.4 - 11.7 vs. 11.0 kgC m^{-2}), and at EucFACE biomass matched well in LPJ-GUESS (12.1 vs. 12.7 kgC m^{-2}) but was low in ED2 (5.6 kgC m^{-2}). Both models also had similar LAI to observations at Palo Verde (3.3 – 4.5 vs. 3.8 (± 1.06) m^2 m^{-2}), and at EucFACE LAI matched well in ED2 (1.6 vs. 1.7 m^2 m^{-2}), but was high for LPJ-GUESS (3.2 m^2 m^{-2}). At EucFACE LAI ranged from 1.2 to 2.1 over a 28-month measurement period (Duursma et al., (2016), but LPJ-GUESS had very large fluctuations in annual LAI outside of these ranges (Fig. S1). These models are well documented and investigated VDMs, with many studies that have looked into parameter uncertainty (see Supplemental Text A for select references that explore model/parameter sensitivity).

Both models displayed nonlinear responses to drought, in concurrence with Hypothesis H1, but they differ in their behavior and between sites. In general, ED2 shows sensitivity to drought duration (Hypothesis H1b), while LPJ-GUESS shows a stronger sensitivity to drought intensity (Hypothesis H1a). ED2's sensitivity to the duration of drought was mild at Palo Verde (Fig. 2a), and stronger at EucFACE particularly during the 4-year drought with a strong non-monotonic pattern (see explanation below) (Fig. 2b). When reporting only percentage of biomass loss, ED2 predicts close to no UCE response at Palo Verde; with a maximum biomass reduction of only 40% during 95% precipitation removal and a 4-year drought event (i.e., UCE). LPJ-GUESS shows no sensitivity to drought duration but is highly sensitive to drought intensity. C loss predicted by LPJ-GUESS at Palo Verde reached a threshold at ~65% drought intensity, after which forests exhibit strong biomass losses, up to 100% (Fig. 2a). At the EucFACE site, both models predict a critical threshold of biomass loss at 35%-45% drought intensity, with LPJ-GUESS predicting total biomass loss (up to 100%) after this drought intensity threshold (Fig. 2b). The EucFACE drought threshold is lower than that of the seasonally dry mixed tropical forest in Palo Verde.

With respect to C loss over a recovering time period (integrated-C-loss), the two models predict similar drought responses at Palo Verde (Fig. 2c), but not at EucFACE (Fig. 2d). At Palo Verde, the similarity between models in integrated-C-loss reflected longer biomass recovery time but less biomass loss in the short-term in ED2 relative to LPJ-GUESS, which predicted greater

biomass loss immediately after drought but shorter recovery time. With the exception of the 1-year drought in ED2, both models predict similar integrated-C-loss across a range of UCEs at Palo Verde, via different pathways. The integrated-C-loss metric revealed a strong non-linear response to drought duration in ED2 (Fig. 2c), while this nonlinearity is less evident when only examining change in biomass (Fig. 2a). The "V"-shaped patterns observed particularly in Fig. 2b, arise from interactions between whole-leaf phenology and stomatal responses to drought in ED2. For drought intensities lower than 40%, stomatal conductance is reduced but leaves are not fully shed. Leaf respiration continues, gradually depleting non-structural C pools, followed by a loss of biomass. However, for higher drought intensities, leaf water potentials quickly become systematically lower than leaf turgor loss points and tree cohorts shed all their leaves. This strategy represents an immediate loss of C via leaf shedding, but spares the cohort from slow, respiration-driven depletion of C stocks.

3.1 Predicted model responses to UCE droughts combined with increased temperature and/or eCO_2

Relating to our second hypothesis of additional effects of warming and eCO_2, we tested 15 treatments in total, repeating the five climate change scenarios for each of the three drought durations. With the addition of climate change impacts, ED2 remained sensitive to the duration of drought, with warming negatively impacting integrated-C-change and most consistently during 2- and 4-year drought durations. ED2 predicts that during the 2- and 4-year droughts at EucFACE, losses are exacerbated when accompanied with warming and even with eCO_2, with 800 ppm having a more detrimental impact than 600 ppm (Fig. 3a-c). The average integrated-C-change was -111.0 kg C m^{-2} yr across all 15 treatments (Table 2). Only during the 1-year drought duration did drought plus warming and eCO_2 have a buffering effect on C stocks, seen in four out of our five scenarios but only during relatively modest droughts intensities (Fig. 3a; i.e., positive integrated-C-change, see also Table 2).

The ED2 simulations of the seasonally dry Palo Verde site (Fig. 3d-f), produced less frequent negative impacts on drought and climate change driven C losses compared to EucFACE, with an average integrated-C-change of -53.9 kg C m^{-2} yr^{-1} across all 15 treatments (Table 2). During the 2-year drought, applying +2K with eCO_2 to 600 ppm showed a slight buffering effect to droughts and the most consistent positive integrated-C-change (Fig. 3e; Table

2). Interestingly, an increase in only eCO_2 to 800 ppm (no warming) when applied with the 2- and 4-year droughts resulted in the largest loss in integrated-C-change (Fig. 3e-f), larger than the expected 'most severe' scenario; +2K and 800 ppm.

Similar to ED2, the LPJ-GUESS model showed a nearly complete negative response in integrated-C-change as a result of UCE drought and scenarios of warming and eCO_2 at the EucFACE site (Fig. 3g-i), but mixed and more muted results at Palo Verde (Fig. 3j-l, Table 2). The average integrated-C-change relative to the reference case was -95.4 at EucFACE and -7.8 kg C m^{-2} yr at Palo Verde, both less negative compared to ED2. One notable pattern was up until a drought intensity threshold of ~40%, the climate scenarios had no effect or response in integrated-C-change at EucFACE, and the muted response from warming and eCO_2 Palo Verde, compared to ED2. Surprisingly, the +2K scenario switched the integrated-C-change to positive, compared to the reference case (Fig. 3g-i; red lines), potentially a physiological process in the model to increased temperatures only that signals an anomalous resiliency response. Similar to the results with no climate change, LPJ-GUESS remained sensitive to the intensity of drought, with ~40% precipitation reduction being a threshold.

The models and sites differed with regard to SO and MO responses to increasing drought severity and its interactions with warming and eCO_2 (related to conceptual Fig. 1d). ED2 showed a more consistent MO response during UCEs and with additional warming and eCO_2 (Fig. 3; negative integrated-C-change), especially at EucFACE, suggesting these ecosystems will remain in a depressed carbon condition driving vegetation mortality, and/or longer recoveries. LPJ-GUESS produced more opportunities for SO with climate change. For example, at EucFACE CO_2 fertilization created small SO periods that then led to MO with increasing drought severities, and at Palo Verde all +2K and 600 ppm led to a SO (Fig. 3j-l; Table 2).

Both models predicted that C losses due to drought interactions with increased temperature and eCO_2 were less severe at the seasonally dry Palo Verde site compared to the somewhat less seasonal, more humid EucFACE site (Table 2), which could be attributed to higher diversity in PFT physiology at Palo Verde. Palo Verde's community composition that emerged following drought included either three (LPJ-GUESS) or four (ED2) PFTs, while only a single PFT existed at EucFACE. With rising temperatures under climate change, UCEs will be hotter and drier. Nine out of the twelve simulations with both +2K and 600 ppm CO_2, and all but one +2K and 800 ppm CO_2 produced a negative integrated-C-change, implying stronger C losses

454 and/or longer recovery times when droughts are exacerbated by increasing temperatures (Table
455 2).
456

457 **4 Discussion**

458 Vegetation demographic models (VDMs) allowed us to uniquely explore two hypotheses
459 regarding a range of modeled response of terrestrial ecosystems to unprecedented climate
460 extremes (UCEs), and setting the stage for the following perspectives to help guide future
461 research. Key model results include strong nonlinearities (Hypothesis H1) in C response to
462 extreme drought *intensities* in LPJ-GUESS and alternatively drought *durations* in ED2 (at one of
463 two sites), with differences in thresholds between the two models and ecosystems. These
464 nonlinearities may arise from multiple mechanisms that we begin to investigate here, including
465 shifts in plant hydraulics or other functional traits, C allocation, phenology, and stand
466 demography, all which vary among ecosystem types. The models also show exacerbated biomass
467 loss and recovery times in the majority of our scenarios of warming and eCO_2, supporting
468 Hypothesis H2. Below, we discuss the underlying mechanisms that drive simulated ecosystem
469 response to UCEs using the models and sites as conceptual "experimental tools" and
470 observational evidence from the literature. We focus on two temporal stages of the UCE: The
471 pre-drought ecosystem stage characterized as the quasi-stable state of the ecosystem prior to a
472 UCE, which can mediate ecosystem resistance and disturbance impact, and the post-drought
473 recovery stage (Table 1).
474

475 **4.1 The role of ecosystem processes and states prior to UCEs**

476 **4.1.1 The role of phenology and phenological strategies prior to UCEs:**

477 Observations show that different levels of deciduousness contribute to alternative
478 strategies for tropical tree response to water stress (Williams et al., 2008). For example, during
479 the severe 1997 El Nino drought, brevi-deciduous trees and deciduous stem-succulents within a
480 tropical dry site in Guanacaste Costa Rica retained leaves during the extreme wet-season
481 drought, behaving differently than during normal dry seasons (Borchert et al., 2002). Both
482 models here predict that neither seasonal deciduousness, nor drought-deciduous phenology at the
483 seasonally dry tropical forest, Palo Verde (which consists of trees with different leaf

phenological strategies), act to buffer the forest from a large drop in LAI during UCEs (Fig. S1a-b). Even with this large decrease in LAI, ED2 predicted a very weak biomass loss at the time of UCEs (Fig. 2a), suggesting large-scale leaf loss is not a direct mechanism of plant mortality in ED2. At the EucFACE site prior to the simulated extreme drought, LAI was stable in ED2, while LPJ-GUESS displayed strong inter-annual variability in LAI (Fig. S1a-b). This capability of large swings in LAI (5.8 to 0.8) by LPJ-GUESS could contribute to model uncertainty and the considerable mortality response at EucFACE. Modeled LAI was the largest source of variability in another ecosystem model, CABLE, when evaluating the simulated response to CO_2 fertilization (Li et al., 2018). Models might better capture the different plant phenological responses to UCEs if the PFT phenology schemes better represented morphological and physiological characteristics relevant to plant-water relations (e.g., leaf age; retention of young leaves even during extreme droughts; Borchert et al., (2002); variation in hydraulic traits as a function of leaf habit Vargas et al., (2021)) (Table 3).

4.1.2 The role of plant hydraulics prior to UCEs:

Susceptibility of plants to hydraulic stress is one of the strongest determinants of vulnerability to drought, with loss of hydraulic conductivity being a major predictor of drought mortality in temperate (McDowell et al., 2013; Anderegg et al., 2015; Sperry and Love, 2015; Venturas et al., 2021) and tropical forests (Rowland et al., 2015; Adams et al., 2017b), as well as a tractable mortality mechanism to represent in process-based models (Choat et al., 2018, Kennedy et al., 2019). Both LPJ-GUESS and ED2 exhibited a wide range in amount and pattern of plant-available-water prior to drought (Fig. S1c-d), leading to large differences in UCE response. LPJ-GUESS predicted lower total plant-available-water at both sites compared to ED2, and subsequently simulated a greater increase in plant-available-water right after the UCEs as a result of greater mortality and decrease in water demand. Due to ED2 using a static mortality threshold from conductivity loss (88%), it likely does not accurately reproduce the wide range of observations of drought-induced mortality. In ED2, large trees, with longer distances to transport water, were at higher risk and suffered higher mortality (Fig. 4), demonstrating how stand demography and size structure can play an important role in ecosystem models (Fisher et al., 2018). There are strong interdependencies and related mechanisms connecting both hydraulic failure (e.g., low soil moisture availability) and C limitation (e.g., stomatal closure) during

515 drought (McDowell et al., 2008; Adams et al., 2017b), and these interactions should be
516 incorporated in ecosystem modeling and further explored (Table 3).

517 **4.1.3. The role of carbon allocation prior to UCEs:**

518 Plants have a variety of strategies to buffer vulnerability to water and nutrient stress
519 caused by extreme droughts, such as allocating more C to deep roots (Joslin et al., 2000; Schenk
520 and Jackson, 2005), investing in mycorrhizal fungi (Rapparini and Peñuelas, 2014), or reducing
521 leaf area without shifting leaf nutrient content (Pilon et al., 1996). Alternatively, presence of
522 deep roots doesn't necessarily lead to deep soil moisture utilization, as seen in a 6-year
523 Amazonian throughfall exclusion experiment where deep root water uptake was still limited,
524 even with high volumetric water content (Markewitz et al., 2010). Elevated CO_2 alone will
525 enhance growth and water-use efficiency (Keenan et al., 2013), reducing susceptibility to
526 drought. However, such increased productivity within a forest stand, and associated structural
527 overshoot during favorable climate windows, can also be reversed by increased competition for
528 light, nutrients, and water during unfavorable UCEs – potentially leading to mortality overshoot
529 (Fig. 1d) and higher C loss. Mortality overshoot could be an explanation for the negative
530 integrated-C-change (i.e., C loss) in the majority of eCO_2-only simulations (18 out of 24
531 scenarios; Table 2).

532 Effects of CO_2 fertilization on plant C allocation strategies are uncertain. As a result,
533 ecosystem models differ in their assumptions on controls of C allocation in response to eCO_2,
534 leading to divergent plant C use efficiencies (Fleischer et al., 2019). Global scale terrestrial
535 models are beginning to include dynamic C allocation schemes, over fixed ratios, that account
536 for concurrent environmental constraints on plants, such as water, and adjust allocation based on
537 resource availability (Weng et al., 2015; Zhu et al., 2019), but the representation of C allocation
538 is still debated and progressing (De Kauwe et al., 2014; Montané et al., 2017; Reyes et al., 2017).
539 It is worth investigating the differences between C allocation based on the allometric partitioning
540 theory (i.e., allocation follows a power allometry function between plant size and organs which
541 is insensitive to environmental conditions; Niklas, 1993), as an alternative to ratio-based optimal
542 partitioning theory (i.e., allocation to plant organs based on the most limiting resources)
543 (McCarthy and Enquist, 2007) or fixed ratios (Table 3), particularly due to VDMs substantial use
544 of allometric relationships. A meta-analysis of 164 studies found that allometric partitioning

theory outperformed optimal partitioning theory in explaining drought-induced changes in C allocation (Eziz et al., 2017).

4.1.4 The role of plant carbon storage prior to UCEs:

Studies of neotropical and temperate seedlings show that pre-drought storage of non-structural carbohydrates (NSCs) provides the resources needed for growth, respiration osmoregulation, and phloem transport when stomata close during subsequent periods of water stress (Myers and Kitajima, 2007; Dietze and Matthes, 2014; O'Brien et al*.,* 2014). Furthermore, direct correlations have been shown between NSC depletion and embolism accumulation, and the degree of pre-stress reserves and utilization of soluble sugars (Tomasella et al., 2020). The amount of NSC storage required to mitigate plant mortality during C starvation and interactions with hydraulic failure from severe drought is difficult to quantify, due to the many roles of NSCs in plant function and metabolism (Dietze and Matthes, 2014). For example, NSCs were not depleted after 13 years of experimental drought in the Brazilian Amazon (Rowland et al., 2015). As atmospheric CO_2 increases with climate change, NSC concentrations may increase, as seen in manipulation experiments (Coley, 2002), but interactions with heat, water stress, enhanced leaf shedding, and nutrient limitation complicates this relationship, and needs to be further explored. Despite the recognition of the critical role that plant hydraulic functioning and NSCs play in tree resilience to extremes, knowledge gaps and uncertainties preclude fully incorporating these processes into ecosystem models.

Compared to ED2, LPJ-GUESS predicted low plant carbon storage (a model proxy for NSCs) prior to and during drought, and at times became negative, thereby creating C costs (Fig. S2a-b), leading to C starvation and potentially explaining the larger biomass loss in LPJ-GUESS at both sites. Alternatively, ED2 maintained higher levels of NSCs providing a buffer to stress, and mitigating the negative effects of drought. Maintenance of NSCs in ED2, even during prolonged drought (at EucFACE) is due to: (1) trees resorbing a fraction of leaf C during leaf shedding, (2) no maintenance costs for NSC storage in the current version, and (3) no allocation of NSCs to structural growth until NSC storage surpasses a threshold (the amount of C needed to build a full canopy of leaves and associated fine roots), allowing for a buffer to accumulate. In LPJ-GUESS, accumulation and depletion of NSC is recorded as a 'C debt' being paid back in later years. The contrasting responses of the two models to drought, and the likely role of NSCs

576 in explaining differences in model behavior, highlights the need to better understand NSC
577 dynamics and to accurately represent the relevant processes in models (Richardson et al., 2013;
578 Dietze and Matthes, 2014). More observations of C accumulation patterns and how/where NSCs
579 drive growth, respiration, transport and cellular water relations would enable a more realistic
580 implementation of NSC dynamics in models (Table 3).
581

582 **4.1.5 Role of functional trait diversity prior to UCEs:**

583 Currently LPJ-GUESS simulates the Palo Verde community using three PFTs, while ED2 uses
584 four PFTs that differ in photosynthetic and hydraulic traits. The community composition simulated by
585 ED2 is shown to be more resistant to UCEs compared to LPJ-GUESS (Fig. 5), perhaps due to
586 relatively higher functional diversity (via more PFTs with additional phenological and hydraulic
587 diversity). This additional diversity helps to buffer ecosystem response to drought by allowing more
588 tolerant PFTs to benefit from reductions in less-tolerant PFTs, thus buffering reductions in ecosystem
589 function (Anderegg et al., 2018). Higher diversity ecosystems were found to protect individual species
590 from negative effects of drought (Aguirre et al., 2021) and enhance productivity resilience following
591 wildfire (Spasojevic et al., 2016); thus, functionally diverse communities may be key to enhancing
592 tolerance to rising environmental stress.

593 Recent efforts to consolidate information on plant traits (Reich et al., 2007; Kattge et al., 2011)
594 have contributed to identifying relationships that can impact community-level drought responses
595 (Skelton et al., 2015; Anderegg et al., 2016a; Uriarte et al., 2016; Greenwood et al., 2017), such as
596 life-history characteristics, and strategies of resource acquisition and conservation as predictors of
597 ecosystem resistance (MacGillivray et al., 1995; Ruppert et al., 2015). While adding plant trait
598 complexity in ESMs may be required to accurately simulate key vegetation dynamics, it necessitates
599 more detailed parameterizations of processes that are not explicitly resolved (Luo et al., 2012). Further
600 investigation of how VDMs represent interactions leading to functional diversity shifts is crucial to
601 this issue. Enquist and Enquist, (2011), as an example, show that long-term patterns of drought (20-
602 years) have led to increases in drought-tolerant dry forest species, which could modulate resistance to
603 future droughts. Higher diversity of plant physiological traits and drought-resistance strategies is
604 expected to enhance community resistance to drought, and models should account for shifts in diverse
605 functionality (Table 3).
606

4.2 The role of ecosystem processes and states in post-UCE recovery

4.2.1 The role of soil water resources post-UCEs:

Our simulation results generally demonstrated a fast recovery of plant-available-water and LAI at both sites (Fig. S1). Annual plant-available-water substantially increased right after drought by an average of 163 mm at Palo Verde and 213 mm at EucFACE in the LPJ-GUESS simulations, compared to much lower increases in ED2 (50 mm and 12 mm at Palo Verde and EucFACE). This increase in available water post-drought can be attributed to reduced stand density and water competition (Fig. S2c-d; diamonds vs. circles), alleviating the demand for soil resources (water) and subsequent stress, which has also been shown in observations (McDowell et al., 2006; D'Amato et al., 2013). After large canopy tree mortality events there can be relatively rapid recovery of forest biogeochemical and hydrological fluxes (Biederman et al., 2015; Anderegg et al., 2016b; Biederman et al., 2016). These crucial fluxes strongly influence plant regeneration and regrowth, which can buffer ecosystem vulnerability to future extreme droughts. However, this enhanced productivity has a limit. In a scenario where UCEs continue to intensify, causing greater reductions in soil water and reduced ecosystem recovery potential, the SO growth that typically occurs after UCEs may be dampened (Fig. 1d). In water-limited locations, similar to the dry forest sites used here, initial forest recovery from droughts were faster due to thinning induced competitive-release of the surviving trees, and shallow roots not having to compete with neighboring trees for water, allowing for more effective water user (Tague and Moritz, 2019), stressing the importance of root competition and distribution in models (Goulden and Bales, 2019). Tague and Moritz, (2019) also reported that this increased water use efficiency and SO ultimately lead to water stress and related declines in productivity, similar to the MO concept (Jump et al., 2017; McDowell et al., 2006). Since a core strength of VDMs is predicting stand demography during recovery, improved quantification of density-dependent competition following stand dieback would be beneficial for model benchmarking (Table 3).

4.2.2 The role of lagged turnover and secondary stressors post-UCEs:

Time lags in forest compositional response and survival to drought could indicate community resistance or shifts to more competitive species and competitive exclusion. During a

637 15-year recovery period from extreme drought at Palo Verde, LPJ-GUESS predicted an increase
638 in stem density (stems m^2 yr^{-1}) (Fig. S2c) compared to ED2, which predicted almost no impact in
639 stem recovery. The mortality "spike" in ED2 due to drought was muted and slightly delayed,
640 contributing to ED2's lower biomass loss and more stable behavior of plant processes over time
641 at Palo Verde. At EucFACE, both models exhibited a pronounced lag effect in stem turnover
642 response, i.e. ~8-12 years after drought (Fig. S2d). After about a decade, strong recoveries and
643 increased stem density occurred, which in ED2 was followed by delayed mortality/thinning of
644 stems. Delayed tree mortality after droughts is common due to optimizing carbon allocation and
645 growth (Trugman et al., 2018), but typically only up to several years post-drought, not a decade
646 or more as seen in the model.

647 The versions of the VDMs used here do not directly consider post-drought secondary
648 stressors such as infestation by insects or pathogens, and the subsequent repair costs due to stress
649 damage, which could substantially slow the recovery of surviving trees. Forest ecologists have
650 long recognized the susceptibility of trees under stress, particularly drought, to insect attacks and
651 pathogens (Anderegg et al., 2015). Tight connections between drought conditions and increased
652 mountain pine beetle activity have been observed (Chapman et al., 2012; Creeden et al., 2014),
653 and can ultimately lead to increased tree mortality (Hubbard et al., 2013). Leaf defoliation is a
654 major concern from insect outbreaks following droughts, and can have large impacts on C
655 cycling, plant productivity, and C sequestration (Amiro et al., 2010; Clark et al., 2010; Medvigy
656 et al., 2012). Implementing these secondary stressors in models could slow the rate of post-UCE
657 recovery and lead to increased post-UCEs tree mortality.

658

659 **4.2.3 The role of stand demography post-UCEs:**

660 Change in stand structure is an important model process to capture, because large trees
661 have important effects on C storage, community resource competition, and hydrology
662 (Wullschleger et al., 2001) (Table 3), and maintaining a positive carbohydrate balance is
663 beneficial in sustaining (or repairing) hydraulic viability (McDowell et al., 2011). There is
664 increasing evidence, both theoretical (McDowell and Allen, 2015) and empirical (Bennett et al.,
665 2015; Rowland et al., 2015; Stovall et al., 2019), that large trees (particularly tall trees with high
666 leaf area) contribute to the dominant fraction of dead biomass after drought events. Under rising

temperatures (and decreasing precipitation), VPD will increase, leading to a higher likelihood of large tree death (Eamus et al., 2013; Stovall et al., 2019), driving MO events as hypothesized in Fig. 1d. Consistent with this expectation, ED2 predicted that the largest trees (>100 cm) experienced the largest decreases in basal area to compared to all other size classes (Fig. 4). This drought-induced partial dieback and whole-tree mortality of dominant trees has substantial impacts on stand-level C dynamics, as long-term sequestered C is liberated during the decay of new dead wood (Palace et al., 2008; Potter et al., 2011). In ED2, the intermediate size class (60 - 80 cm) increased in basal area following large-tree death, taking advantage of the newly open canopy space. However, small size classes do not necessarily benefit from canopy dieback. For example, in a dry tropical forest, prolonged drought led to a decrease in understory species and small-sized stems (Enquist and Enquist, 2011).

4.2.4 The role of functional trait diversity & plant hydraulics post-UCEs:

During the recovery phase from disturbance, competition will likely shift the plant community towards one that is composed of opportunistic, fast-growing pioneer tree species, grasses (Shiels et al., 2010; Carreño-Rocabado et al., 2012), and/or deciduous species, as also seen in previous model results (Hickler et al., 2004). In the treatments presented here, deciduous PFT types were also the strongest to recover after 15 years in both models, surpassing pre-drought values (Fig. 5). It should be noted that ED2 exhibited a strong recovery in the evergreen PFT as well (over two other deciduous PFT types), inconsistent with the above literature (Fig. 5b). PFTs in ED2 respond to drought conditions via stomatal closure and leaf shedding, buffering stem water potentials from falling below a set mortality threshold (i.e., 88% of loss in conductivity). This conductivity threshold may need to be reconsidered if further examination reveals an unrealistic advantage under drought conditions for evergreen trees, which exhibited a lower impact from droughts (compared to deciduous and brevi-deciduous PFTs) in ED2.

Recovery of surviving trees could be hindered by the high cost of replacing damaged xylem associated with cavitation (McDowell et al., 2008; Brodribb et al., 2010). Many studies have identified “drought legacy” effects of delayed growth or gross primary productivity following drought (Anderegg et al., 2015; Schwalm et al., 2017) and the magnitude of these legacies across species correlates with the hydraulic risks taken during drought itself (Anderegg

et al., 2015). The conditions under which xylem can be refilled remain controversial, but it seems likely that many species, particularly gymnosperms, may need to entirely replace damaged xylem (Sperry et al., 2002), and trees worldwide operate within narrow hydraulic safety margins, suggesting that trees in all biomes are vulnerable to drought (Choat et al., 2012). The amount of damaged xylem from a given drought event and recovery rates also vary across trees of different sizes (Anderegg et al., 2018).

Plasticity in nutrient acquisition traits, intraspecific variation in plant hydraulic traits (Anderegg et al., 2015), and changes in allometry (e.g., Huber values) can have large effects on acclimation to extreme droughts. This suggests some capacity for physiological adaptation to extreme drought, as seen by short-term negative effects from drought and heat extremes being compensated for in the longer term (Dreesen et al., 2014). Still, given the shift towards more extreme droughts with climate change, vegetation mortality thresholds are likely to be exceeded, as reported in Amazonian long-term plots where mortality of wet-affiliated genera has increased while simultaneously new recruits of dry-affiliated genera are also increasing (Esquivel-Muelbert et al., 2019). Increasing occurrences of heat events, water stress and high VPD will lead to extended closure of stomata to avoid cavitation, progressively reducing CO_2 enrichment benefits (Allen et al., 2015). Where CO_2 fertilization has been seen to partially offset the risk of increasing temperatures, the risk response was mediated by plant hydraulic traits (Liu et al., 2017), yet interactions with novel extreme droughts were not considered. The VDM simulations suggest that the combination of elevated warming and eCO_2 will exacerbate consequences of UCEs by reductions in both C stocks and post-drought biomass recovery speeds (Fig. 3). Therefore, future UCE recovery may not be easily predicted from observations of historical post-disturbance recovery. An associated area for further investigation is to better understand the hypothesized interplay between amplified mortality from hotter UCEs followed by structural overshoot regrowth during wetter periods (Fig. 1d), which could potentially lead to continual large swings in MO and SO and vulnerable net ecosystem C fluxes through time (Table 3).

5 Summary of perspectives for model advancement

Model limitations and unknowns exposed by our simulations and literature review highlight current challenges in our ability to understand and forecast UCE effects on ecosystems. These limitations reflect a general lack of empirical experiments focused on UCEs. Insufficient

data means that relevant processes may currently be poorly represented in models, and models may then misrepresent C losses during UCEs. The two VDMs used here had different sensitivities to drought duration and intensity. These model uncertainties could potentially be addressed by improved datasets on thresholds of conductivity loss at high drought intensities, the role of trait diversity (e.g., different strategies of drought deciduousness) in buffering ecosystem drought responses, and a better grasp of plant storage stocks before, during, and after multi-year droughts. Our study takes some initial steps to identify and assess model uncertainties in terms of mechanisms and magnitudes of responses to UCEs, which can then be used to inform and develop field experiments targeting key knowledge gaps as well as to prioritize ongoing model development (Table 3). Our intention was not to do an exhaustive list of UCE simulation experiments, and outstanding modeling perturbations and experiments would be useful outcomes of future studies. This iterative model-experiment framework of using VDMs as hypothesis testing tools offers strong potential to drive progress in improving our understanding of terrestrial ecosystem responses to UCEs and climate feedbacks, while informing the development of the next generation of models.

Code Availability. The source code for the ED2 model can be downloaded and available publicly at https://github.com/EDmodel/ED2. The source code for the LPJ-GUESS model can be downloaded and available publicly at http://web.nateko.lu.se/lpj-guess/download.html. All model simulation data will be available in a Dryad repository.

Data Availability. Authors received the required permissions to use the site level meteorological data used in this study. Otherwise, no ecological or biological data were used in this study.

Author Contributions. JH wrote the manuscript with significant contributions from AR, BS, JD, DM, with input and contributions from all authors. XX and MM were the primary leads running the model simulations, with model assistance and strong feedback from DM and BS. All authors made contributions to this article, and agree to submission.

Competing Interests. The contact author has declared that neither they nor their co-authors have any competing interests.

Special Issue Statement. Special Issue titled "Ecosystem experiments as a window to future carbon, water, and nutrient cycling in terrestrial ecosystems"

Financial Support: Funding for the meetings that facilitated this work was provided by NSF-DEB-0955771: An Integrated Network for Terrestrial Ecosystem Research on Feedbacks to the Atmosphere and ClimatE (INTERFACE): Linking experimentalists, ecosystem modelers, and Earth System modelers, hosted by Purdue University; as well as Climate Change Manipulation Experiments in Terrestrial Ecosystems: Networking and Outreach (COST action ClimMani – ES1308), led by the University of Copenhagen. J.A. Holm's time was supported as part of the Next Generation Ecosystem Experiments-Tropics, funded by the U.S. Department of Energy, Office of Science, Office of Biological and Environmental Research under Contract DE-AC02-05CH11231. AR acknowledges funding from CLIMAX Project funded by Belmont Forum and the German Federal Ministry of Education and Research (BMBF). BS and MM acknowledge support from the Strategic Research Area MERGE. W.R.L.A. acknowledges funding from the University of Utah Global Change and Sustainability Center, NSF Grant 1714972, and the USDA National Institute of Food and Agriculture, Agricultural and Food Research Initiative Competitive Programme, Ecosystem Services and Agro-ecosystem Management, grant no. 2018-67019-27850. JL acknowledges support from the Northern Research Station of the USDA Forest Service (agreement 16-JV-11242306-050) and a sabbatical fellowship from sDiv, the Synthesis Centre of iDiv (DFG FZT 118, 202548816). CDA acknowledges support from the USGS Land Change Science R&D Program.

Acknowledgements. We thank Belinda Medlyn and David Ellsworth of the Hawkesbury Institute for the Environment, Western Sydney University, for providing the meteorological forcing data series for the EucFACE site, a facility supported by the Australian Government through the Education Investment Fund and the Department of Industry and Science, in partnership with Western Sydney University.

Table 1. Hypothesized plant processes and ecosystem state variables affecting pre-drought resistance and post-drought recovery in the context of unprecedented climate extremes (UCEs). The "Included in Model?" column indicates which processes or state variables are represented in each of the two models studied in this paper. Mechanisms listed in the two right columns refer to real ecosystems and are not necessarily represented in models, even if the process or state variable is represented in a given model. Contents of the table are based on a non-exhaustive literature review, expert knowledge, and modeling results presented here. Symbols refer to the following literature sources: * Borchert et al., 2002; Williams et al., (2008); ** Dietze and Matthes, (2014); O'Brien et al., 2014; *** ENQUIST and ENQUIST, (2011); Greenwood et al., (2017); Powell et al., (2018); ^ Rowland et al., (2015); McDowell et al., (2013); Anderegg et al., (2015); ^^ Joslin et al., 2000; Markewitz et al., (2010); ^^^ Powell et al., (2018); ^^^^ Bennett et al., (2015); Rowland et al., (2015); ~ Hubbard et al., (2013); ~ ~ McDowell et al., 2006, D'Amato et al., (2013); + Vargas et al., (2021).

Process or State Variable	Included in model?	Mechanisms affecting pre-UCE drought resistance influencing impact	Mechanisms affecting post-UCE drought recovery
Processes			
1) Phenology Schemes	ED2: Yes LPJ-G: Yes	Leaf area and metabolic activity modulate vulnerability to death; drought-deciduousness reduces vulnerability to drought *, with higher water potential at turgor loss point and leaf vulnerability to embolism +	Leaf lifespan tends to increase from pioneer to late-successional species in some ecosystems (e.g., tropical forests)
2) Plant Hydraulics	ED2: Yes LPJ-G: No	Cavitation resistance traits ^; turgor loss, hydraulic failure (stem embolism) lead to increased plant mortality and enhanced vulnerability to secondary stressors	Replacement cost of damaged xylem slows recovery of surviving trees
3) Dynamic Carbon Allocation	ED2: Yes LPJ-G: Yes	Increased root allocation could offset soil water deficit under gradual onset of drought ^^	Allocation among fine roots, xylem, & leaves affects recovery time & GPP/LAI trajectory

4) Non-Structural Carbohydrate (NSC) Storage	ED2: Yes LPJ-G: Yes	Buffers C starvation mortality due to reduced primary productivity; maintenance of hydraulic function & avoiding hydraulic failure **	Low NSC could increase vulnerability to secondary stressors during recovery
State Variables			
1) Plant-Soil Water Availability	ED2: Yes LPJ-G: Partly	Low soil water potential increases risk of tree C starvation, turgor loss and hydraulic failure	After stand dieback reduced demand for soil resources &/or reduced shading. Increased soil water enhances regeneration/ regrowth, buffers vulnerability to long-term drought ~ ~
2) Plant Functional Diversity	ED2: Yes LPJ-G: Yes	Presence of drought-tolerant species modulates resistance at community level. Shallow-rooting species more vulnerable ^^^ ***	Changed resource spectra shift competitive balance in favor of grasses and pioneer trees
3) Stand Demography	ED2: Yes LPJ-G: Yes	Larger tree size enhances vulnerability to drought and secondary stressors due to higher maintenance costs ^^^^	Mortality of canopy individuals favors understory species and smaller size-classes
4) Compounding Stressors	ED2: No LPJ-G: No	Reduced resistance to insects and pathogens due to physiological/mechanical/ hydraulic damage & depletion of NSC	Infestation by insects and pathogens, repair of damage due to secondary stressors, slows recovery of surviving trees ~

800

Table 2 Impact of eCO_2 and/or temperature on the integrated-C-change (kg C m^{-2} yr) relative to drought treatments with no additional warming or eCO_2, for both models, and both sites seen in Fig. 3. Quantified as average and minimum integrated-C-change across all 20 drought intensities for step-change scenarios of warming and eCO_2. The percentage of each scenario that was negative in integrated-C-change (i.e., decreases in C loss). Green values represent positive integrated-C-change.

EucFACE		*ED2*			*LPJ-GUESS*		
		Average integrated C change	Largest integrated C change	% climate scenario was negative	Average integrated C change	Largest integrated C change	% climate scenario was negative
1 year	600 ppm	**2.2**	0.0	33.3	-74.6	-396.6	36.8
	800 ppm	-10.6	-73.0	50.0	-124.1	-416.0	57.9
	2K	**2.3**	-0.5	16.7	**21.3**	-20.8	15.8
	2K, 600 ppm	**0.5**	-8.2	61.1	-67.5	-201.5	78.9
	2K, 800 ppm	**1.8**	-0.4	22.2	-145.9	-400.1	47.4
2 year	600 ppm	-105.6	-456.7	77.8	-85.2	-260.6	63.2
	800 ppm	-199.0	-522.9	83.3	-106.3	-350.1	42.1
	2K	-10.3	-34.7	77.8	**14.2**	-35.2	31.6
	2K, 600 ppm	-204.9	-666.1	77.8	-47.6	-128.8	84.2
	2K, 800 ppm	-12.4	-61.6	50.0	-167.0	-421.9	68.4
4 year	600 ppm	-125.5	-306.2	83.3	-122.6	-277.4	94.7
	800 ppm	-277.1	-423.3	100.0	-212.2	-523.7	89.5
	2K	-61.8	-188.6	72.2	**12.9**	-13.8	31.6
	2K, 600 ppm	-385.9	-674.2	94.4	-79.1	-197.3	94.7
	2K, 800 ppm	-277.9	-737.7	72.2	-247.0	-503.8	100.0
	Average	-111.0	-277.0	64.8	-95.4	-276.5	62.5
Palo Verde		*ED2*			*LPJ-GUESS*		
1 year	600 ppm	-1.6	-6.2	77.8	-11.0	-32.4	78.9
	800 ppm	**6.7**	-0.2	11.1	-39.2	-154.0	100.0
	2K	-1.0	-15.3	38.9	-33.4	-75.1	100.0
	2K, 600 ppm	**2.5**	-1.1	22.2	**6.5**	-4.6	52.6
	2K, 800 ppm	-6.6	-16.6	77.8	-121.1	-237.7	100.0
2 year	600 ppm	**15.1**	-16.7	38.9	**27.3**	-6.0	10.5
	800 ppm	-229.2	-756.6	66.7	**20.6**	-17.2	26.3
	2K	-8.2	-71.8	50.0	**32.0**	-12.7	15.8
	2K, 600 ppm	**24.8**	-5.7	11.1	**36.2**	-1.2	5.3
	2K, 800 ppm	-152.9	-348.1	77.8	**8.0**	-54.5	36.8
4 year	600 ppm	-11.1	-37.3	94.4	**3.4**	-25.1	26.3
	800 ppm	-260.2	-694.8	94.4	-25.2	-132.6	57.9
	2K	-39.0	-133.8	66.7	-7.7	-45.9	68.4
	2K, 600 ppm	**1.0**	-16.4	38.9	**6.1**	-4.1	31.6
	2K, 800 ppm	-148.5	-429.3	83.3	-20.0	-75.5	78.9
	Average	-53.9	-170.0	56.7	-7.8	-58.6	52.6

Table 3 Summary of suggestions emerging from the hypothetical drought simulations used here of the driving mechanisms (e.g., ecosystem or plant processes and state variables) to explore for future research in manipulation experiments, data collection, and model development and testing, as related to furthering our understanding of UCE resistance and recovery.

	UCE Drought Resistance & Recovery Summary
Processes	**Suggestions of driving mechanisms to further explore in data and models**
1) Phenology Schemes	Represent morphological and physiological traits relevant to plant-water relations; drought- deciduousness can reduce vulnerability to drought; phenology of evergreens needs more investigation.
2) Plant Hydraulics	Interactions between hydraulic failure (e.g. low soil moisture availability) and C limitation (e.g. stomatal closure) during drought should be included in models. Account for turgor loss, hydraulic failure traits, costs to recover damaged xylem.
3) Dynamic Carbon Allocation	C allocation based on the allometric partitioning theory in addition, or replacing ratio-based optimal partitioning theory, and fixed ratios. Explore root allocation that could offset soil water deficits.
4) Non-structural Carbohydrate (NSC) Storage	Deciding best practices for NSC representation in models. Better understanding of NSC storage required to mitigate plant mortality during C starvation and interactions with avoiding hydraulic failure during severe droughts.
States Variables	
1) Plant-Soil Water Availability	Better quantification of the amount and accessibility of plant-available water for surviving trees, and tradeoff between increased structural productivity but vulnerability to subsequent droughts. Future relevance, or benefit, of lower water demand due to thinning with UCEs.
2) Plant Functional Diversity	Understand how higher diversity of plant physiological traits and drought-resistance strategies will enhance community resistance to drought; models still need to account for shifts in diverse functionality, including deciduousness shifts and interplay of regrowth structural overshoot followed by amplified mortality from hotter UCEs.
3) Stand Demography	Large trees more vulnerable to drought; need data on changes in C stock with UCEs in high-density smaller tree stands vs. stands with larger trees.

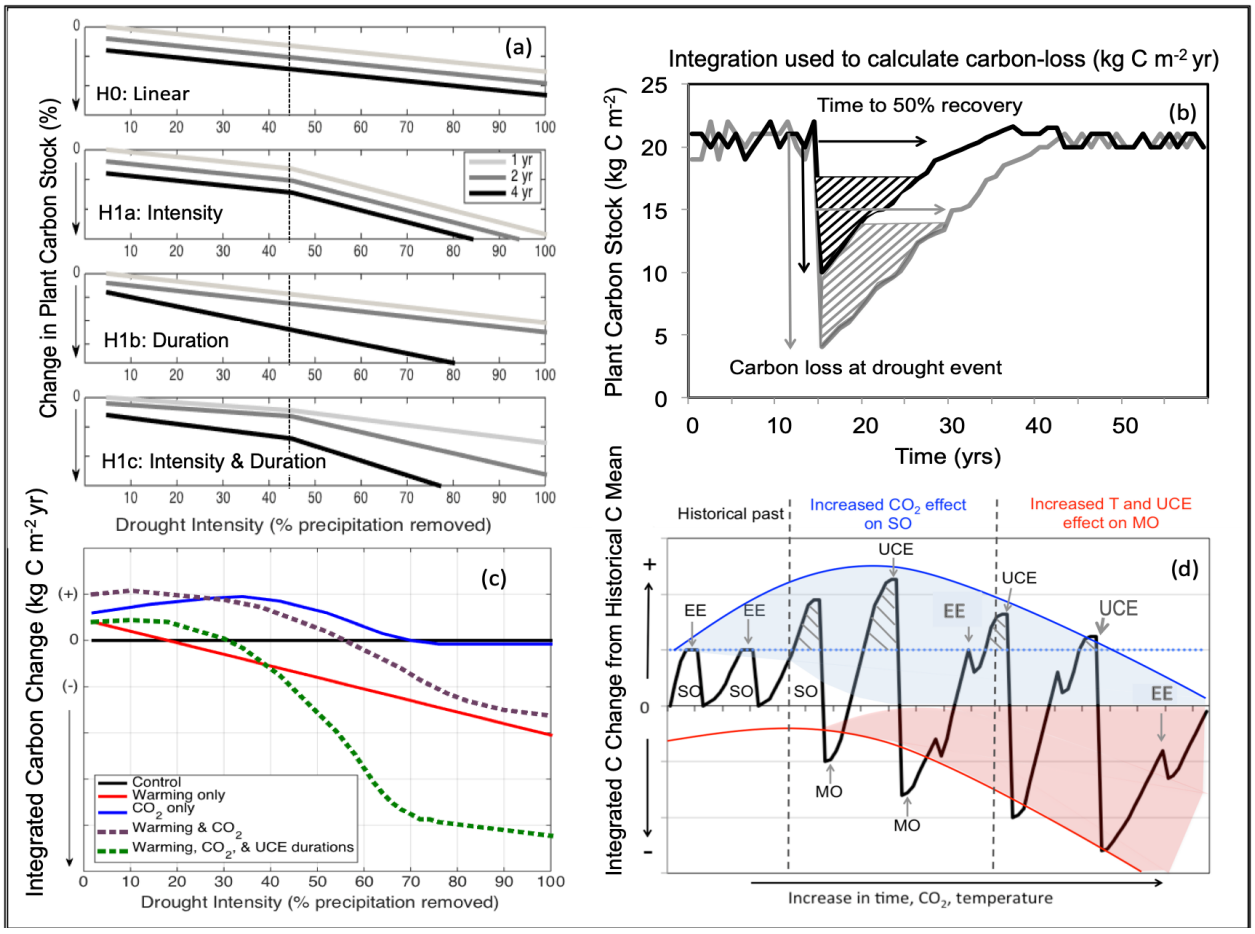

Figure 1 Conceptual diagrams showing impacts of extreme droughts (unprecedented climate extremes, UCEs; i.e., record-breaking droughts) on plant C stocks. (a) **Conceptual response diagram**: potential loss in C stock as a function of increasing drought intensity (0-100% precipitation removal) and drought duration (1, 2 or 4 years of drought). In this example, an arbitrary threshold of 45% precipitation reduction and 4-year drought duration is assumed to correspond to a UCE. The "null hypothesis" (H0, top panel) is a linear response of C stocks to droughts. Alternative hypotheses include nonlinear and threshold responses to drought intensity (H1a), drought duration via different slope responses (H1b), and combined effects of both drought intensity and durations (H1c). (b) **Conceptualized UCE C loss diagram**: responses of forest C stocks to a large (grey) and small (black) UCE. "Integrated-C-loss" (kg C m^{-2} yr) denotes the integral of the C loss over time and is calculated from the two arrows: the total loss in C (kg C m^{-2}) due to drought, and the time (yr) to recover 50% of the pre-drought C stock. (c) **Conceptualized UCE-climate C change diagram:** hypothetical response in terrestrial

828 "integrated-C-change" (kg C m^{-2} yr) due to eCO_2 (blue line), rising temperature (red line),
829 interaction between eCO_2 and temperature (dashed purple), and combined interactions among
830 eCO_2, temperature, and UCEs of prolonged durations (green line), all relative to a reference
831 drought of normal duration with no warming (black line). Integrated-C-change denotes the
832 difference in integrated-C-loss (see panel b) between a scenario of changing climatic drivers and
833 the reference drought (control). (d) **Conceptual UCE amplification diagram**: hypothetical
834 amplified change in forest C stocks to eCO_2 and temperature relative to the pre-warming
835 historical past (based on Jump et al. (2017)). Change in C stock greater than zero indicates a
836 'structural overshoot' (SO) due to favorable environmental conditions and/or recovery from an
837 extreme drought-heat event (EE). Hashed black areas indicate a structural overshoot due to
838 eCO_2, which occurs over the historical CO_2 levels (dashed blue line). Initially, an eCO_2 effect
839 leads to a larger increase in structural overshoot (due to CO_2 fertilization), driving more extreme
840 vegetation mortality ('mortality overshoot' - MO) relative to historical dieback events and thus a
841 greater decrease in C stock. Increased warming through time increasingly counteracts any CO_2
842 fertilization effect; while the amplitude of post-UCE C stock recoveries remains large, net C
843 stock values eventually decline (downward curvature) due to more pronounced loss in C stocks
844 (and greater ecosystem state change) from hotter UCEs.
845 SO = structural overshoot, MO = mortality overshoot, EE = historically extreme drought-heat
846 event, UCE = unprecedented climate extreme.
847

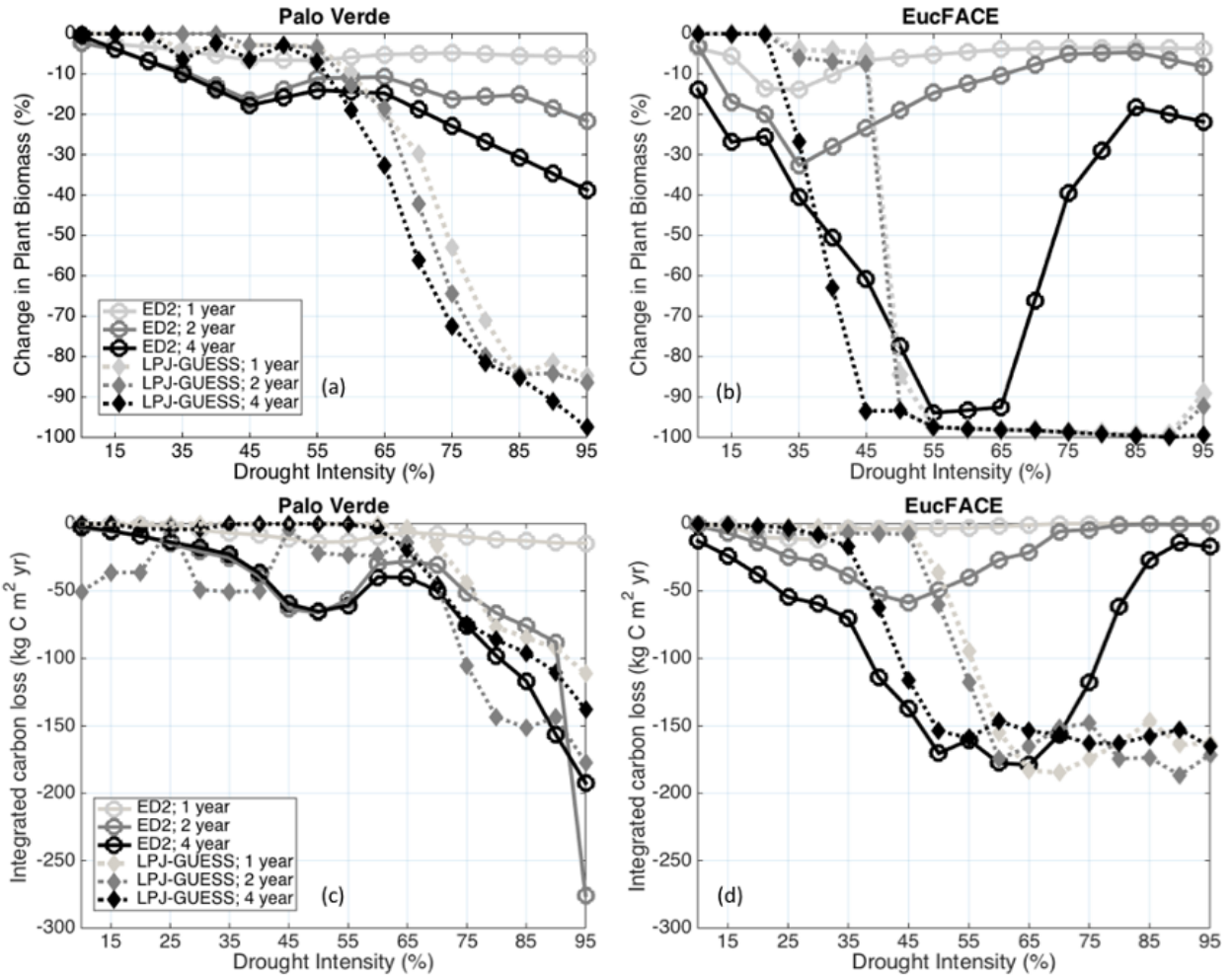

848

849 **Figure 2** Modeled change in biomass (%) at the end of drought periods of different lengths (1, 2,
850 and 4-year droughts) and intensities (up to 95% precipitation removed) at (a) Palo Verde, and (b)
851 EucFACE, for the ED2 and LPJ-GUESS models. Modeled integrated-C-loss (C reduction due to
852 extreme drought integrated over time until biomass recovers to 50% of the non-drought baseline
853 biomass) at (c) Palo Verde and (d) EucFACE.

854

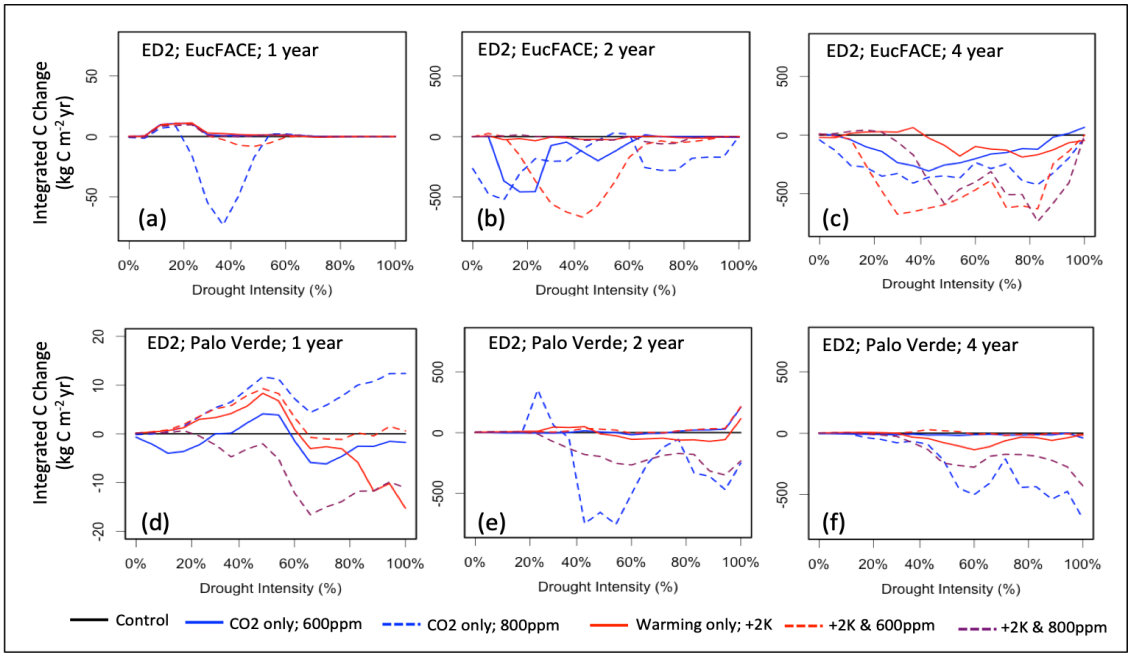

855

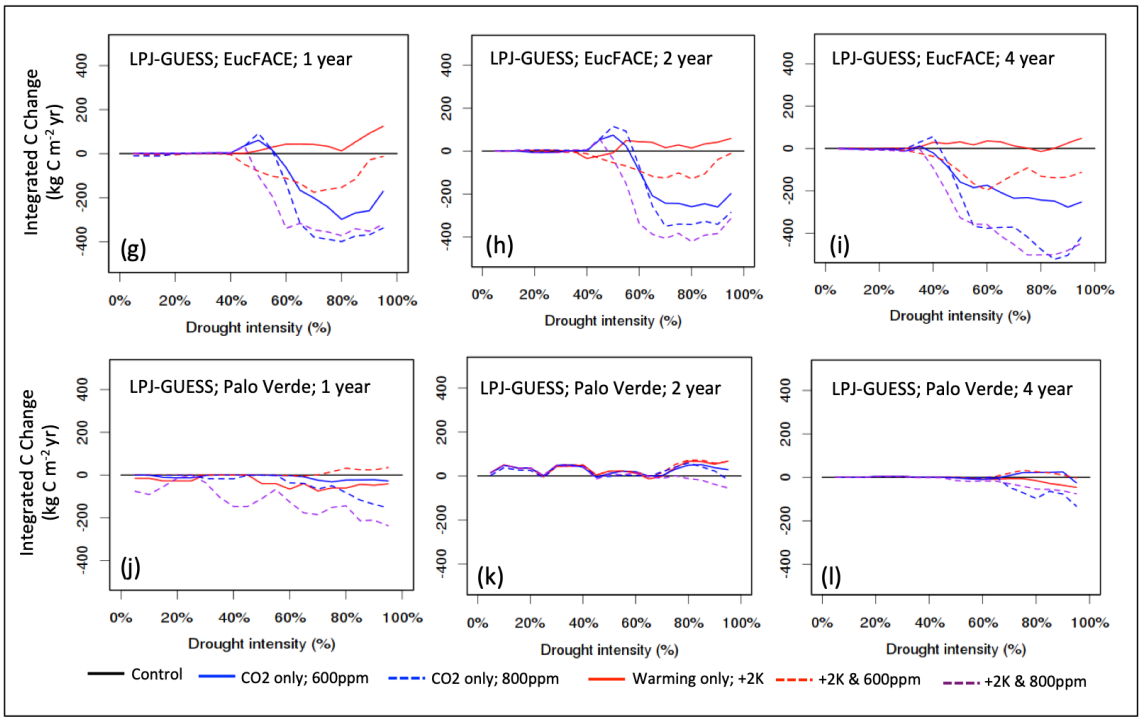

856

857 **Figure 3** Vegetation C response to interactions between drought intensity (0% to 100%
858 precipitation reduction), drought durations (1, 2, 4-year droughts), and idealized scenarios of
859 warming and eCO_2 compared to the reference simulation, simulated by two VDMs; ED2 (a-f)
860 and LPJ-GUESS (g-l) at two sites (EucFACE and Palo Verde). The scenarios include a control
861 (current temperature; 400 ppm atmospheric CO_2), two eCO_2 scenarios (600 ppm or 800 ppm),

elevated temperature (2 K above current), and a combination of eCO_2 (600 ppm or 800 ppm) and higher temperature. Vegetation response is quantified as "integrated-C-change" (in kg C m^{-2} yr; Eq. 4), which is defined as the difference in integrated-C-losses due to drought between a given scenario of change in climatic drivers and the control. Negative values for integrated-C-change indicate that warming and/or eCO_2 leads to stronger C losses and/or longer recovery, while positive values for integrated-C-change indicates a buffering effect.

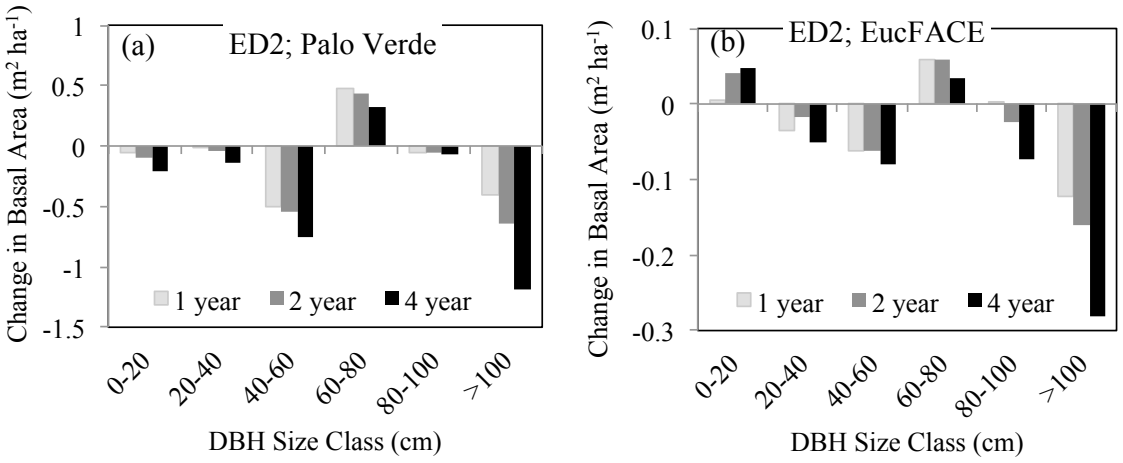

Figure 4 Change in basal area (m^2 ha^{-1}) immediately following either 1, 2, or 4 year droughts for six increasing size class bins (DBH, cm) as predicted by the ED2 model for (a) the Palo Verde site, with 90% precipitation removed, and (b) the EucFACE site with 50% precipitation removed.

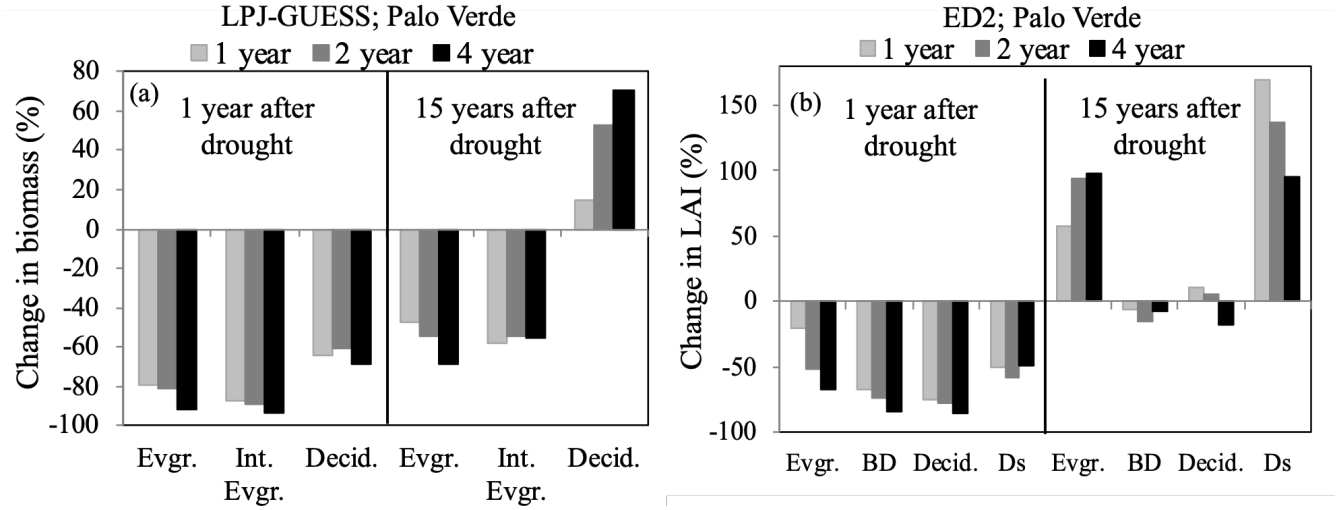

Figure 5 Percent change in community composition, represented by plant functional type (PFT), the year following three drought durations of UCEs (1, 2, and 4-year droughts and 90% precipitation removed) as well as 15 years after droughts, for the tropical Palo Verde site by (a) LPJ-GUESS reported in biomass change, and (b) ED2 reported in LAI change. Even though Ds had the strongest recovery, it should be noted it was the least abundant PFT at this site. Evgr. = evergreen, Int. Ever. = intermediate evergreen, Decid. = deciduous, BD = brevi-deciduous, Ds = deciduous stem-succulent. EucFACE data not shown because only one PFT present (evergreen tree).

References:

Adams, H.D., Guardiola-Claramonte, M., Barron-Gafford, G.A., Villegas, J.C., Breshears, D.D., Zou, C.B. et al.: Temperature sensitivity of drought-induced tree mortality portends increased regional die-off under global-change-type drought, PNAS, 106, 7063-7066, 2009.

Adams, H.D., Barron-Gafford, G.A., Minor, R.L., Gardea, A.A., Bentley, L.P., Law, D.J. et al.: Temperature response surfaces for mortality risk of tree species with future drought, Environ. Res. Lett., 12, 115014, 2017a.

Adams, H.D., Zeppel, M.J.B., Anderegg, W.R.L., Hartmann, H., Landhäusser, S.M., Tissue, D.T. et al.: A multi-species synthesis of physiological mechanisms in drought-induced tree mortality, Nature Ecol. & Evol., 1, 1285-1291, 2017b.

Aguirre, BA, Hsieh, B, Watson, SJ, Wright, AJ.: The experimental manipulation of atmospheric drought: Teasing out the role of microclimate in biodiversity experiments, J. Ecol., 109, 1986– 1999, https://doi.org/10.1111/1365-2745.13595, 2021.

Ahlström, A., Schurgers, G., Arneth, A. & Smith, B.: Robustness and uncertainty in terrestrial ecosystem carbon response to CMIP5 climate change projections, Environ. Res. Lett., 7, 044008, 2012.

Ainsworth, E.A. & Long, S.P.: What have we learned from 15 years of free-air CO2 enrichment (FACE)? A meta-analytic review of the responses of photosynthesis, canopy properties and plant production to rising CO2, New Phytol., 165, 351-372, 2005.

Allen, C.D., Breshears, D.D. & McDowell, N.G.: On underestimation of global vulnerability to tree mortality and forest die-off from hotter drought in the Anthropocene, Ecosphere, 6, art129, 2015.

Allen, K., Dupuy, J.M., Gei, M.G., Hulshof, C.M., Medvigy, D., Pizano, C. et al.: Will seasonally dry tropical forests be sensitive or resistant to future changes in 558 rainfall regimes? Environ. Res. Lett., 12, 023001, 2017.

Amiro, B.D., Barr, A.G., Barr, J.G., Black, T.A., Bracho, R., Brown, M. et al.: Ecosystem carbon dioxide fluxes after disturbance in forests of North America, J. Geophys. Res. Biogeosciences, 115, 2010.

Anderegg, W.R.L., Hicke, J.A., Fisher, R.A., Allen, C.D., Aukema, J., Bentz, B. et al.: Tree mortality from drought, insects, and their interactions in a changing climate, New Phytol., 208, 674-683, 2015.

Anderegg, W.R.L., Klein, T., Bartlett, M., Sack, L., Pellegrini, A.F.A., Choat, B. et al.: Meta-analysis reveals that hydraulic traits explain cross-species patterns of drought-induced tree mortality across the globe, PNAS, 113, 5024-5029, 2016a.

Anderegg, W.R.L., Martinez-Vilalta, J., Cailleret, M., Camarero, J.J., Ewers, B.E., Galbraith, D. et al.: When a Tree Dies in the Forest: Scaling Climate-Driven Tree Mortality to Ecosystem Water and Carbon Fluxes, Ecosystems, 19, 1133-1147, 2016b.

Anderegg, W.R.L., Konings, A.G., Trugman, A.T., Yu, K., Bowling, D.R., Gabbitas, R. et al.: Hydraulic diversity of forests regulates ecosystem resilience during drought, Nature, 561, 538-541, 2018.

Asner, G.P., Brodrick, P.G., Anderson, C.B., Vaughn, N., Knapp, D.E. & Martin, R.E.: Progressive forest canopy water loss during the 2012–2015 California drought. PNAS, 113, E249-E255, 2016.

930 Arora, V.K., Katavouta, A., Williams, R.G., Jones, C.D., Brovkin, V., Friedlingstein, P., et al.:
931 Carbon-concentration and carbon-climate feedbacks in CMIP6 models and their
932 comparison to CMIP5 models, Biogeosciences, 17, 4173–4222, 2020.
933 Bai, Y., Wu, J., Xing, Q., Pan, Q., Huang, J., Yang, D. et al.: PRIMARY PRODUCTION AND
934 RAIN USE EFFICIENCY ACROSS A PRECIPITATION GRADIENT ON THE
935 MONGOLIA PLATEAU, Ecology, 89, 2140-2153, 2008.
936 Beier, C., Beierkuhnlein, C., Wohlgemuth, T., Penuelas, J., Emmett, B., Körner, C. et al.:
937 Precipitation manipulation experiments – challenges and recommendations for the future,
938 Ecol. Lett., 15, 899-911, 2012.
939 Bennett, A.C., McDowell, N.G., Allen, C.D. & Anderson-Teixeira, K.J.: Larger trees suffer most
940 during drought in forests worldwide, Nature Plants, 1, 15139, 2015.
941 Biederman, J.A., Meixner, T., Harpold, A.A., Reed, D.E., Gutmann, E.D., Gaun, J.A. et al.:
942 Riparian zones attenuate nitrogen loss following bark beetle-induced lodgepole pine
943 mortality, J. Geophys. Res. Biogeosciences, 121, 933-948, 2016.
944 Biederman, J.A., Somor, A.J., Harpold, A.A., Gutmann, E.D., Breshears, D.D., Troch, P.A. et al.:
945 Recent tree die-off has little effect on streamflow in contrast to expected increases from
946 historical studies, Water Resources Res., 51, 9775-9789, 2015.
947 Blyth, E.M., Arora, V.K., Clark, D.B. et al.: Advances in Land Surface Modelling, Curr. Clim.
948 Change Rep., 7, 45–71, https://doi.org/10.1007/s40641-021-00171-5, 2021.
949 Borchert, R., Rivera, G. & Hagnauer, W.: Modification of Vegetative Phenology in a Tropical
950 Semi-deciduous Forest by Abnormal Drought and Rain, Biotropica, 34, 27-39, 2002.
951 Brando, P.M., Paolucci, L., Ummenhofer, C.C., Ordway, E.M., Hartmann, H., Cattau, M.E.,
952 Rattis, L., Medjibe, V., Coe, M.T., Balch, J.: Droughts, Wildfires, and Forest Carbon
953 Cycling: A Pantropical Synthesis, Annual Review of Earth and Planetary Sciences, 47, 555-
954 581, 2019.
955 Breshears, D.D., Myers, O.B., Meyer, C.W., Barnes, F.J., Zou, C.B., Allen, C.D. et al.: Tree die-
956 off in response to global change-type drought: mortality insights from a decade of plant
957 water potential measurements, Front. Ecol. Environ., 7, 185-189, 2009.
958 Brodribb, T.J., Bowman, D.J.M.S., Nichols, S., Delzon, S. & Burlett, R.: Xylem function and
959 growth rate interact to determine recovery rates after exposure to extreme water deficit, New
960 Phytol., 188, 533-542, 2010.
961 Carreño-Rocabado, G., Peña-Claros, M., Bongers, F., Alarcón, A., Licona, J.-C. & Poorter, L.:
962 Effects of disturbance intensity on species and functional diversity in a tropical forest, J.
963 Ecology, 100, 1453-1463, 2012.
964 Chapman, T.B., Veblen, T.T. & Schoennagel, T.: Spatiotemporal patterns of mountain pine beetle
965 activity in the southern Rocky Mountains, Ecology, 93, 2175-2185, 2012.
966 Chiang, F., Mazdiyasni, O. & AghaKouchak, A.: Evidence of anthropogenic impacts on global
967 drought frequency, duration, and intensity, Nat Commun., 12**,** 2754,
968 https://doi.org/10.1038/s41467-021-22314-w, 2021.
969 Choat, B., Brodribb, T.J., Brodersen, C.R., Duursma, R.A., López, R. & Medlyn, B.E.: Triggers
970 of tree mortality under drought, Nature, 558, 531-539, 2018.
971 Choat, B., Jansen, S., Brodribb, T.J., Cochard, H., Delzon, S., Bhaskar, R. et al.: Global
972 convergence in the vulnerability of forests to drought, Nature, 491, 752-755, 2012.
973 Christoffersen, B.O., Gloor, M., Fauset, S., Fyllas, N.M., Galbraith, D.R., Baker, T.R. et al.:
974 Linking hydraulic traits to tropical forest function in a size-structured and trait-driven model
975 (TFS v.1-Hydro), Geosci. Model Dev. Discuss., 2016, 1-60, 2016.

Ciais, P., Reichstein, M., Viovy, N., Granier, A., Ogée, J., Allard, V. et al.: Europe-wide reduction in primary productivity caused by the heat and drought in 2003, Nature, 437, 529, 2005.
Ciais, P., Sabine, C., Bala, G., Bopp, L., Brovkin, V., Canadell, J., et al.: Carbon and other biogeochemical cycles. In: Climate Change 2013: The Physical Science Basis. Contribution of Working Group I to the Fifth Assessment Report of the Intergovernmental Panel on Climate Change (eds. Stocker, T.F., Qin, D., Plattner, G.-K., Tignor, M., Allen, S.K., Boschung, J., et al.), Cambridge University Press, Cambridge, United Kingdom and New York, NY, USA, pp. 465–570, 2013.
Clark, K.L., Skowronski, N. & Hom, J.: Invasive insects impact forest carbon dynamics, Glob. Change Biol., 16, 88-101, 2010.
Coley, P., Massa, M., Lovelock, C., Winter, K.: Effects of elevated CO2 on foliar chemistry of saplings of nine species of tropical tree, Oecologia, 2002.
Creeden, E.P., Hicke, J.A. & Buotte, P.C.: Climate, weather, and recent mountain pine beetle outbreaks in the western United States, Forest Ecol. Manag., 312, 239-251, 2014.
D'Amato, A.W., Bradford, J.B., Fraver, S. & Palik, B.J.: Effects of thinning on drought vulnerability and climate response in north temperate forest ecosystems, Eco. Applications, 23, 1735-1742, 2013.
da Costa, A.C.L., Galbraith, D., Almeida, S., Portela, B.T.T., da Costa, M., de Athaydes Silva Junior, J. et al., Effect of 7 yr of experimental drought on vegetation dynamics and biomass storage of an eastern Amazonian rainforest, New Phytol., 187, 579-591, 2010.
De Kauwe, M.G., Medlyn, B.E., Zaehle, S., Walker, A.P., Dietze, M.C., Wang, Y.-P. et al.: Where does the carbon go? A model-data intercomparison of vegetation carbon allocation and turnover processes at two temperate forest free-air CO2 enrichment sites, New Phytol, 203, 883-899, 2014.
Dietze, M.C. & Matthes, J.H.: A general ecophysiological framework for modelling the impact of pests and pathogens on forest ecosystems, Ecol. Lett., 17, 1418-1426, 2014.
Döscher, R., Acosta, M., et al.: The EC-Earth3 Earth System Model for the Climate Model Intercomparison Project 6, Geosci. Model Dev. Discuss. [preprint], https://doi.org/10.5194/gmd-2020-446, in revision, 2022.
Dreesen, F.E., De Boeck, H.J., Janssens, I.A. & Nijs, I.: Do successive climate extremes weaken the resistance of plant communities? An experimental study using plant assemblages, Biogeosciences, 11, 109-121, 2014.
Duursma, R.A., Gimeno, T.E., Boer, M.M., Crous, K.Y., Tjoelker, M.G. and Ellsworth, D.S.: Canopy leaf area of a mature evergreen *Eucalyptus* woodland does not respond to elevated atmospheric [CO_2] but tracks water availability, Glob. Change Biol., 22, 1666-1676, https://doi.org/10.1111/gcb.13151, 2016.
Eamus, D., Boulain, N., Cleverly, J. & Breshears, D.D.: Global change-type drought-induced tree mortality: vapor pressure deficit is more important than temperature per se in causing decline in tree health, Ecol. Evol., 3, 2711-2729, 2013.
Ellsworth, David S., Anderson, Ian C., Crous, Kristine Y., Cooke, J., Drake, John E., Gherlenda, Andrew N. et al.: Elevated CO2 does not increase eucalypt forest productivity on a low-phosphorus soil, Nature Climate Change, 7, 279, 2017.
ENQUIST, B.J. & ENQUIST, C.A.F.: Long-term change within a Neotropical forest: assessing differential functional and floristic responses to disturbance and drought, Glob. Change Biol., 17, 1408-1424, 2011.

Esquivel-Muelbert, A., Baker, T.R., Dexter, K.G., Lewis, S.L., Brienen, R.J.W., Feldpausch, T.R. et al.: Compositional response of Amazon forests to climate change, Glob. Change Biol., 25, 39-56, 2019.
Eziz, A., Yan, Z., Tian, D., Han, W., Tang, Z. & Fang, J.: Drought effect on plant biomass allocation: A meta-analysis, Ecol. Evol, 7, 11002-11010, 2017.
Feldpausch, T.R., Phillips, O.L., Brienen, R.J.W., Gloor, E., Lloyd, J., Lopez-Gonzalez, G. et al.: Amazon forest response to repeated droughts, Global Biogeochemical Cycles, 30, 964-982, 2016.
Fisher, R.A., Muszala, S., Verteinstein, M., Lawrence, P., Xu, C., McDowell, N.G. et al.: Taking off the training wheels: the properties of a dynamic vegetation model without climate envelopes, CLM4.5(ED), Geosci. Model Dev., 8, 3593-3619, 2015.
Fisher, R.A., Koven, C.D., Anderegg, W.R.L., Christoffersen, B.O., Dietze, M.C., Farrior, C.E. et al.: Vegetation demographics in Earth System Models: A review of progress and priorities, Glob. Change Biol., 24, 35-54, 2018.
Fisher, R. A., and Koven, C. D.: Perspectives on the future of land surface models and the challenges of representing complex terrestrial systems, JAMES, 12, e2018MS001453, https://doi.org/10.1029/2018MS001453, 2020.
Fleischer, K., Rammig, A., De Kauwe, M.G., Walker, A.P., Domingues, T.F., Fuchslueger, L. et al.: Amazon forest response to CO2 fertilization dependent on plant phosphorus acquisition, Nature Geoscience, 12, 736-741, 2019.
Frank, D., Reichstein, M., Bahn, M., Thonicke, K., Frank, D., Mahecha, M.D. et al.: Effects of climate extremes on the terrestrial carbon cycle: concepts, processes and potential future impacts, Glob. Change Biol., 21, 2861-2880, 2015.
Friend, A.D., Lucht, W., Rademacher, T.T., Keribin, R., Betts, R., Cadule, P. et al.: Carbon residence time dominates uncertainty in terrestrial vegetation responses to future climate and atmospheric CO2, PNAS, 111, 3280-3285, 2014.
Gerten, D., LUO, Y., Le MAIRE, G., PARTON, W.J., KEOUGH, C., WENG, E. et al.: Modelled effects of precipitation on ecosystem carbon and water dynamics in different climatic zones, Glob. Change Biol., 14, 2365-2379, 2008.
Goulden, M.L. & Bales, R.C.: California forest die-off linked to multi-year deep soil drying in 2012–2015 drought, Nature Geoscience, 12, 632-637, 2019.
Gray, S.B., Dermody, O., Klein, S.P., Locke, A.M., McGrath, J.M., Paul, R.E. et al.: Intensifying drought eliminates the expected benefits of elevated carbon dioxide for soybean, Nature Plants, 2, 16132, 2016.
Greenwood, S., Ruiz-Benito, P., Martínez-Vilalta, J., Lloret, F., Kitzberger, T., Allen, C.D. et al.: Tree mortality across biomes is promoted by drought intensity, lower wood density and higher specific leaf area, Ecol. Lett., 20, 539-553, 2017.
Griffin, D. & Anchukaitis, K.J.: How unusual is the 2012–2014 California drought? Geophys. Res. Lett., 41, 9017-9023, 2014.
Hickler, T., Smith, B., Sykes, M.T., Davis, M.B., Sugita, S. & Walker, K.: USING A GENERALIZED VEGETATION MODEL TO SIMULATE VEGETATION DYNAMICS IN NORTHEASTERN USA, Ecology, 85, 519-530, 2004.
Holm, J. A., Knox, R. G., Zhu, Q., Fisher, R. A., Koven, C. D., Nogueira Lima, A. J., et al.: The central Amazon biomass sink under current and future atmospheric CO_2: Predictions from big-leaf and demographic vegetation models, J. Geophys. Res. Biogeosciences, 125, e2019JG005500. https://doi.org/10.1029/2019JG005500, 2020.

Hovenden, M.J., Newton, P.C.D. & Wills, K.E.: Seasonal not annual rainfall determines grassland biomass response to carbon dioxide, Nature, 511, 583, 2014.
Hubbard, R.M., Rhoades, C.C., Elder, K. & Negron, J.: Changes in transpiration and foliage growth in lodgepole pine trees following mountain pine beetle attack and mechanical girdling, Forest Ecol. Manag., 289, 312-317, 2013.
IPCC: Managing the Risks of Extreme Events and Disasters to Advance Climate Change Adaptation. A Special Report of Working Groups I and II of the Intergovernmental Panel on Climate Change. (ed. Field, C.B., V. Barros, T.F. Stocker, D. Qin, D.J. Dokken, K.L. Ebi, M.D. Mastrandrea, K.J. Mach, G.-K. Plattner, S.K. Allen, M. Tignor, and P.M. Midgley) Cambridge, UK, and New York, NY, USA, p. 582 pp, 2012.
IPCC: Climate Change 2021: The Physical Science Basis. Contribution of Working Group I to the Sixth Assessment Report of the Intergovernmental Panel on Climate Change [Masson-Delmotte, V., P. Zhai, A. Pirani, S.L. Connors, C. Péan, S. Berger, N. Caud, Y. Chen, L. Goldfarb, M.I. Gomis, M. Huang, K. Leitzell, E. Lonnoy, J.B.R. Matthews, T.K. Maycock, T. Waterfield, O. Yelekçi, R. Yu, and B. Zhou (eds.)]. Cambridge University Press, 2021.
Jiang, M., Medlyn, B.E., Drake, J.E., Duursma, R.A., Anderson, I.C., Barton, C.V.M., Boer, M.B., Carrillo, Y., Castañeda-Gómez, L., Collins, L., et al.: The fate of carbon in a mature forest under carbon dioxide enrichment, Nature, 580, 227-231, https://doi.org/10.1038/s41586-020-2128-9, 2020.
Joslin, J.D., Wolfe, M.H. & Hanson, P.J.: Effects of altered water regimes on forest root systems, New Phytol., 147, 117-129, 2000.
Jump, A.S., Ruiz-Benito, P., Greenwood, S., Allen, C.D., Kitzberger, T., Fensham, R. et al.: Structural overshoot of tree growth with climate variability and the global spectrum of drought-induced forest dieback, Glob. Change Biol., 23, 3742-3757, 2017.
Kalacska, M.E.R., Sánchez-Azofeifa, G.A., Calvo-Alvarado, J.C., Rivard, B. and Quesada, M.: Effects of Season and Successional Stage on Leaf Area Index and Spectral Vegetation Indices in Three Mesoamerican Tropical Dry Forests, Biotropica, 37, 486-496, https://doi.org/10.1111/j.1744-7429.2005.00067.x, 2005.
Kannenberg, S.A., Schwalm, C.R. and Anderegg, W.R.L.: Ghosts of the past: how drought legacy effects shape forest functioning and carbon cycling, Ecol. Lett., 23: 891-901, https://doi.org/10.1111/ele.13485, 2020.
Kattge, J., DÍAZ, S., LAVOREL, S., PRENTICE, I.C., LEADLEY, P., BÖNISCH, G. et al.: TRY – a global database of plant traits, Global Change Biol, 17, 2905-2935, 2011.
Kayler, Z.E., De Boeck, H.J., Fatichi, S., Grünzweig, J.M., Merbold, L., Beier, C. et al.: Experiments to confront the environmental extremes of climate change, Front. Ecol. Environ., 13, 219-225, 2015.
Keenan, T.F., Hollinger, D.Y., Bohrer, G., Dragoni, D., Munger, J.W., Schmid, H.P. et al.: Increase in forest water-use efficiency as atmospheric carbon dioxide concentrations rise, Nature, 499, 324-327, 2013.
Kennedy, D., Swenson, S., Oleson, K. W., Lawrence, D. M., Fisher, R., Lola da Costa, A. C., & Gentine, P.: Implementing plant hydraulics in the Community Land Model, version 5, JAMES, 11, 485– 513. https://doi.org/10.1029/2018MS001500, 2019.
Li, Q., Lu, X., Wang, Y., Huang, X., Cox, P. M., and Luo, Y.: Leaf area index identified as a major source of variability in modeled CO_2 fertilization, Biogeosciences, 15, 6909–6925, https://doi.org/10.5194/bg-15-6909-2018, 2018.

Liu, Y., Parolari, A.J., Kumar, M., Huang, C.-W., Katul, G.G. & Porporato, A.: Increasing atmospheric humidity and CO2 concentration alleviate forest mortality risk, PNAS, 114, 9918-9923, 2017.
Lloret, F., Escudero, A., Iriondo, J.M., Martínez-Vilalta, J. & Valladares, F.: Extreme climatic events and vegetation: the role of stabilizing processes, Glob. Change Biol., 18, 797-805, 2012.
Luo, Y., Gerten, D., Le Maire, G., Parton, W.J., Weng, E., Zhou, X. et al.: Modeled interactive effects of precipitation, temperature, and [CO2] on ecosystem carbon and water dynamics in different climatic zones, Glob. Change Biol., 14, 1986-1999, 2008.
Luo, Y.Q., Randerson, J.T., Abramowitz, G., Bacour, C., Blyth, E., Carvalhais, N. et al.: A framework for benchmarking land models, Biogeosciences, 9, 3857-3874, 2012.
Luo, Y., Jiang, L., Niu, S., Zhou, X.: Nonlinear responses of land ecosystems to variation in precipitation, New Phytol., 214, 5–7, 2017.
MacGillivray, C.W., Grime, J.P. & The Integrated Screening Programme, T.: Testing Predictions of the Resistance and Resilience of Vegetation Subjected to Extreme Events, Funct. Ecol., 9, 640-649, 1995.
Markewitz, D., Devine, S., Davidson, E.A., Brando, P. & Nepstad, D.C.: Soil moisture depletion under simulated drought in the Amazon: impacts on deep root uptake, New Phytol., 187, 592-607, 2010.
Matusick, G., Ruthrof, K.X., Brouwers, N.C., Dell, B. & Hardy, G.S.J.: Sudden forest canopy collapse corresponding with extreme drought and heat in a mediterranean-type eucalypt forest in southwestern Australia, European J. Forest Res., 132, 497-510, 2013.
Matusick, G., Ruthrof, K.X., Fontaine, J.B. & Hardy, G.E.S.J.: Eucalyptus forest shows low structural resistance and resilience to climate change-type drought, J. Vegetation Science, 27, 493-503, 2016.
McCarthy, M.C. & Enquist, B.J.: Consistency between an allometric approach and optimal partitioning theory in global patterns of plant biomass allocation, Funct. Ecol., 21, 713-720, 2007.
McDowell, N., Pockman, W.T., Allen, C.D., Breshears, D.D., Cobb, N., Kolb, T. et al.: Mechanisms of plant survival and mortality during drought: why do some plants survive while others succumb to drought? New Phytol., 178, 719-739, 2008.
McDowell, N.G., Adams, H.D., Bailey, J.D., Hess, M. & Kolb, T.E.: Homeostatic Maintenance Of Ponderosa Pine Gas Exchange In Response To Stand Density Changes, Ecological Applications, 16, 1164-1182, 2006.
McDowell, N.G. & Allen, C.D.: Darcy's law predicts widespread forest mortality under climate warming, Nature Climate Change, 5, 669-672, 2015.
McDowell, N.G., Beerling, D.J., Breshears, D.D., Fisher, R.A., Raffa, K.F. & Stitt, M.: The interdependence of mechanisms underlying climate-driven vegetation mortality, Trends in Ecol. & Evolution, 26, 523-532, 2011.
McDowell, N.G., Fisher, R.A., Xu, C., Domec, J.C., Hölttä, T., Mackay, D.S. et al.: Evaluating theories of drought-induced vegetation mortality using a multimodel–experiment framework, New Phytol., 200, 304-321, 2013.
Medlyn, B.E., De Kauwe, M.G., Zaehle, S., Walker, A.P., Duursma, R.A., Luus, K., Mishurov, M., Pak, B., Smith, B., Wang, Y.-P., Yang, X., Crous, K.Y., Drake, J.E., Gimeno, T.E., Macdonald, C.A., Norby, R.J., Power, S.A., Tjoelker, M.G. & Ellsworth, D.S.: Using

models to guide field experiments: a priori predictions for the CO2 response of a nutrient- and water-limited native Eucalypt woodland, Glob. Change Biol., 22, 2834-2851, 2016.
Medvigy, D., Wang, G., Zhu, Q., Riley, W.J., Trierweiler, A.M., Waring, B., Xu, X. and Powers, J.S.: Observed variation in soil properties can drive large variation in modelled forest functioning and composition during tropical forest secondary succession, New Phytol, 223, 1820-1833, https://doi.org/10.1111/nph.15848, 2019.
Medvigy, D., Clark, K.L., Skowronski, N.S. & Schäfer, K.V.R.: Simulated impacts of insect defoliation on forest carbon dynamics, Environ. Res. Lett., 7, 045703, 2012.
Medvigy, D. & Moorcroft, P.R.: Predicting ecosystem dynamics at regional scales: an evaluation of a terrestrial biosphere model for the forests of northeastern North America, Philosophical Transactions of the Royal Society B: Biological Sciences, 367, 222-235, 2012.
Medvigy, D., Wofsy, S., Munger, J., Hollinger, D. & Moorcroft, P.: Mechanistic scaling of ecosystem function and dynamics in space and time: Ecosystem Demography model version 2, J. Geophys. Res. Biogeosciences, 114, 2009.
Meir, P., Wood, T.E., Galbraith, D.R., Brando, P.M., Da Costa, A.C.L., Rowland, L. et al.: Threshold Responses to Soil Moisture Deficit by Trees and Soil in Tropical Rain Forests: Insights from Field Experiments, BioScience, 65, 882-892, 2015.
Montané, F., Fox, A.M., Arellano, A.F., MacBean, N., Alexander, M.R., Dye, A. et al.: Evaluating the effect of alternative carbon allocation schemes in a land surface model (CLM4.5) on carbon fluxes, pools, and turnover in temperate forests, Geosci. Model Dev., 10, 3499-3517, 2017.
Muldavin, E.H., Moore, D.I., Collins, S.L., Wetherill, K.R. & Lightfoot, D.C.: Aboveground net primary production dynamics in a northern Chihuahuan Desert ecosystem, Oecologia, 155, 123-132, 2008.
Myers, J.A. & Kitajima, K.: Carbohydrate storage enhances seedling shade and stress tolerance in a neotropical forest, J. Ecology, 95, 383-395, 2007.
Niklas, K. J.: The scaling of plant height: A comparison among major plant clades and anatomical grades, Annals of Botany, 72, 165–172, https://doi.org/10.1006/anbo.1993.1095, 1993.
Norby, R.J., DeLucia, E.H., Gielen, B., Calfapietra, C., Giardina, C.P., King, J.S. et al.: Forest response to elevated CO2 is conserved across a broad range of productivity, PNAS, 102, 18052-18056, 2005.
O'Brien, M.J., Leuzinger, S., Philipson, C.D., Tay, J. & Hector, A.: Drought survival of tropical tree seedlings enhanced by non-structural carbohydrate levels, Nature Climate Change, 4, 710, 2014.
Obermeier, W.A., Lehnert, L.W., Kammann, C.I., Müller, C., Grünhage, L., Luterbacher, J. et al.: Reduced CO2 fertilization effect in temperate C3 grasslands under more extreme weather conditions, Nature Climate Change, 7, 137, 2016.
Palace, M., Keller, M. & Silva, H.: NECROMASS PRODUCTION: STUDIES IN UNDISTURBED AND LOGGED AMAZON FORESTS, Ecological Applications, 18, 873-884, 2008.
Phillips, O.L., Aragão, L.E.O.C., Lewis, S.L., Fisher, J.B., Lloyd, J., López-González, G. et al.: Drought Sensitivity of the Amazon Rainforest, Science, 323, 1344-1347, 2009.
Phillips, O.L., van der Heijden, G., Lewis, S.L., López-González, G., Aragão, L.E.O.C., Lloyd, J. et al.: Drought–mortality relationships for tropical forests, New Phytol., 187, 631-646, 2010.
Pilon, C.E., Côté, B. & Fyles, J.W.: Effect of an artificially induced drought on leaf peroxidase activity, mineral nutrition and growth of sugar maple, Plant and Soil, 179, 151-158, 1996.

Potter, C., Klooster, S., Hiatt, C., Genovese, V. & Castilla-Rubio, J.C.: Changes in the carbon cycle of Amazon ecosystems during the 2010 drought, Environ. Res. Lett., 6, 034024, 2011.
Powell, T.L., Galbraith, D.R., Christoffersen, B.O., Harper, A., Imbuzeiro, H.M.A., Rowland, L. et al.: Confronting model predictions of carbon fluxes with measurements of Amazon forests subjected to experimental drought, New Phytol., 200, 350-365, 2013.
Powell, T.L., Koven, C.D., Johnson, D.J., Faybishenko, B., Fisher, R.A., Knox, Ryan G. et al.: Variation in hydroclimate sustains tropical forest biomass and promotes functional diversity, New Phytol., 219, 932-946, 2018.
Powers, J.S., Becknell, J.M., Irving, J. & Pèrez-Aviles, D.: Diversity and structure of regenerating tropical dry forests in Costa Rica: Geographic patterns and environmental drivers, Forest Ecol. Manag., 258, 959-970, 2009.
Powers, J.S. & Peréz-Aviles, D.: Edaphic Factors are a More Important Control on Surface Fine Roots than Stand Age in Secondary Tropical Dry Forests, Biotropica, 45, 1-9, 2013.
Powers, JS, Vargas G., G, Brodribb, TJ, et al.: A catastrophic tropical drought kills hydraulically vulnerable tree species, Glob. Change Biol. 2020; 26: 3122– 3133, https://doi.org/10.1111/gcb.15037, 2020.
Rapparini, F. & Peñuelas, J.: Mycorrhizal Fungi to Alleviate Drought Stress on Plant Growth. In: Use of Microbes for the Alleviation of Soil Stresses, Volume 1 (ed. Miransari, M), Springer New York New York, NY, pp. 21-42, 2014.
Reich, P.B., Hobbie, S.E. & Lee, T.D.: Plant growth enhancement by elevated CO2 eliminated by joint water and nitrogen limitation, Nature Geoscience, 7, 920, 2014.
Reich, P.B., Wright, I.J. & Lusk, C.H.: PREDICTING LEAF PHYSIOLOGY FROM SIMPLE PLANT AND CLIMATE ATTRIBUTES: A GLOBAL GLOPNET ANALYSIS, Ecological Applications, 17, 1982-1988, 2007.
Reichstein, M., Bahn, M., Ciais, P., Frank, D., Mahecha, M.D., Seneviratne, S.I. et al.: Climate extremes and the carbon cycle, Nature, 500, 287-295, 2013.
Reyes, J.J., Tague, C.L., Evans, R.D. & Adam, J.C.: Assessing the Impact of Parameter Uncertainty on Modeling Grass Biomass Using a Hybrid Carbon Allocation Strategy, 9, 2968-2992, 2017.
Richardson, A.D., Carbone, M.S., Keenan, T.F., Czimczik, C.I., Hollinger, D.Y., Murakami, P. et al.: Seasonal dynamics and age of stemwood nonstructural carbohydrates in temperate forest trees, New Phytol., 197, 850-861, 2013.
Rowland, L., da Costa, A.C.L., Galbraith, D.R., Oliveira, R.S., Binks, O.J., Oliveira, A.A.R. et al.: Death from drought in tropical forests is triggered by hydraulics not carbon starvation, Nature, 528, 119, 2015.
Roy, J., Picon-Cochard, C., Augusti, A., Benot, M.-L., Thiery, L., Darsonville, O. et al.: Elevated CO2 maintains grassland net carbon uptake under a future heat and drought extreme, PNAS, 113, 6224-6229, 2016.
Ruppert, J.C., Harmoney, K., Henkin, Z., Snyman, H.A., Sternberg, M., Willms, W. et al.: Quantifying drylands' drought resistance and recovery: the importance of drought intensity, dominant life history and grazing regime, Glob. Change Biol., 21, 1258-1270, 2015.
Rustad, L.E.: The response of terrestrial ecosystems to global climate change: Towards an integrated approach, Science of The Total Environ., 404, 222-235, 2008.
Ruthrof, K.X., Breshears, D.D., Fontaine, J.B., Froend, R.H., Matusick, G., Kala, J. et al.: Subcontinental heat wave triggers terrestrial and marine, multi-taxa responses, Scientific Reports, 8, 13094, 2018.

Scheiter, S., Langan, L. & Higgins, S.I.: Next-generation dynamic global vegetation models: learning from community ecology, New Phytol., 198, 957-969, 2013.
Schenk, H.J. & Jackson, R.B.: Mapping the global distribution of deep roots in relation to climate and soil characteristics, Geoderma, 126, 129-140, 2005.
Schwalm, C.R., Anderegg, W.R.L., Michalak, A.M., Fisher, J.B., Biondi, F., Koch, G. et al.: Global patterns of drought recovery, Nature, 548, 202, 2017.
Seneviratne, S.I., X. Zhang, M. Adnan, W. Badi, C. Dereczynski, A. Di Luca, S. Ghosh, I. Iskandar, J. Kossin, S. Lewis, F. Otto, I. Pinto, M. Satoh, S.M. Vicente-Serrano, M. Wehner, and B. Zhou, 2021: Weather and Climate Extreme Events in a Changing Climate. In Climate Change 2021: The Physical Science Basis. Contribution of Working Group I to the Sixth Assessment Report of the Intergovernmental Panel on Climate Change [Masson-Delmotte, V., P. Zhai, A. Pirani, S.L. Connors, C. Péan, S. Berger, N. Caud, Y. Chen, L. Goldfarb, M.I. Gomis, M. Huang, K. Leitzell, E. Lonnoy, J.B.R. Matthews, T.K. Maycock, T. Waterfield, O. Yelekçi, R. Yu, and B. Zhou (eds.)], Cambridge University Press, Cambridge, United Kingdom and New York, NY, USA, pp. 1513–1766, doi:10.1017/9781009157896.013, 2021.
Settele, J., Scholes, R., Betts, R., Bunn, S.E., Leadley, P., Nepstad, D., Overpeck, J.T., and Taboada, M.A.: Terrestrial and inland water systems. In: Climate Change 2014: Impacts, Adaptation, and Vulnerability. Part A: Global and Sectoral Aspects. Contribution of Working Group II to the Fifth Assessment Report of the Intergovernmental Panel on Climate Change, Cambridge University Press Cambridge, United Kingdom and New York, NY, USA, pp. 271-359, 2014.
Sheffield, J., Goteti, G. & Wood, E.F.: Development of a 50-Year High-Resolution Global Dataset of Meteorological Forcings for Land Surface Modeling, J. Climate, 19, 3088-3111, 2006.
Shiels, A.B., Zimmerman, J.K., García-Montiel, D.C., Jonckheere, I., Holm, J., Horton, D. et al.: Plant responses to simulated hurricane impacts in a subtropical wet forest, Puerto Rico, J. Ecology, 98, 659-673, 2010.
Sippel, S., Zscheischler, J. & Reichstein, M.: Ecosystem impacts of climate extremes crucially depend on the timing, PNAS, 113, 5768-5770, 2016.
Sitch, S., HUNTINGFORD, C., GEDNEY, N., LEVY, P.E., LOMAS, M., PIAO, S.L. et al.: Evaluation of the terrestrial carbon cycle, future plant geography and climate-carbon cycle feedbacks using five Dynamic Global Vegetation Models (DGVMs), Glob. Change Biol., 14, 2015-2039, 2008.
Skelton, R.P., West, A.G. & Dawson, T.E.: Predicting plant vulnerability to drought in biodiverse regions using functional traits, PNAS, 112, 5744-5749, 2015.
Smith, B., Prentice, I.C. & Sykes, M.T.: Representation of vegetation dynamics in the modelling of terrestrial ecosystems: comparing two contrasting approaches within European climate space, Global Ecol. Biogeo., 10, 621-637, 2001.
Smith, B., Wårlind, D., Arneth, A., Hickler, T., Leadley, P., Siltberg, J. et al.: Implications of incorporating N cycling and N limitations on primary production in an individual-based dynamic vegetation model, Biogeosciences, 11, 2027-2054, 2014.
Spasojevic, M.J., Bahlai, C.A., Bradley, B.A., Butterfield, B.J., Tuanmu, M.-N., Sistla, S. et al.: Scaling up the diversity–resilience relationship with trait databases and remote sensing data: the recovery of productivity after wildfire, Glob. Change Biol., 22, 1421-1432, 2016.

1295 Sperry, J.S., Hacke, U.G., Oren, R. & Comstock, J.P.: Water deficits and hydraulic limits to leaf
1296 water supply, Plant, Cell & Environ., 25, 251-263, 2002.
1297 Sperry, J.S. & Love, D.M.: What plant hydraulics can tell us about responses to climate-change
1298 droughts, New Phytol., 207, 14-27, 2015.
1299 Sperry, J.S., Wang, Y., Wolfe, B.T., Mackay, D.S., Anderegg, W.R.L., McDowell, N.G. et al.:
1300 Pragmatic hydraulic theory predicts stomatal responses to climatic water deficits, New
1301 Phytol., 212, 577-589, 2016.
1302 Stovall, A.E.L., Shugart, H. & Yang, X.: Tree height explains mortality risk during an intense
1303 drought, Nature Communications, 10, 4385, 2019.
1304 Tague, C.L. & Moritz, M.A.: Plant Accessible Water Storage Capacity and Tree-Scale Root
1305 Interactions Determine How Forest Density Reductions Alter Forest Water Use and
1306 Productivity, Front. Forests and Global Change, 2, 2019.
1307 Tomasella M, Petrussa E, Petruzzellis F, Nardini A, Casolo V.: The Possible Role of Non-
1308 Structural Carbohydrates in the Regulation of Tree Hydraulics, International Journal of
1309 Molecular Sciences, 21:144, https://doi.org/10.3390/ijms21010144, 2020.
1310 Trugman, A.T., Detto, M., Bartlett, M.K., Medvigy, D., Anderegg, W.R.L., Schwalm, C. et al.:
1311 Tree carbon allocation explains forest drought-kill and recovery patterns, Ecol. Lett., 21,
1312 1552-1560, 2018.
1313 Uriarte, M., Lasky, J.R., Boukili, V.K. & Chazdon, R.L.: A trait-mediated, neighbourhood
1314 approach to quantify climate impacts on successional dynamics of tropical rainforests,
1315 Funct. Ecol., 30, 157-167, 2016.
1316 Vargas G., G., Brodribb, T.J., Dupuy, J.M., González-M., R., Hulshof, C.M., Medvigy, D.,
1317 Allerton, T.A.P., Pizano, C., Salgado-Negret, B., Schwartz, N.B., Van Bloem, S.J., Waring,
1318 B.G. and Powers, J.S.: Beyond leaf habit: generalities in plant function across 97 tropical
1319 dry forest tree species, New Phytol, 232: 148-161. https://doi.org/10.1111/nph.17584, 2021.
1320 Venturas, M. D., Todd, H. N., Trugman, A. T., & Anderegg, W. R.: Understanding and predicting
1321 forest mortality in the western United States using long-term forest inventory data and
1322 modeled hydraulic damage, New Phytol., 230, 1896-1910, 2021.
1323 Wang, D., Heckathorn, S.A., Wang, X. & Philpott, S.M.: A meta-analysis of plant physiological
1324 and growth responses to temperature and elevated CO2, Oecologia, 169, 1-13, 2012.
1325 Weng, E.S., Malyshev, S., Lichstein, J.W., Farrior, C.E., Dybzinski, R., Zhang, T. et al.: Scaling
1326 from individual trees to forests in an Earth system modeling framework using a
1327 mathematically tractable model of height-structured competition, Biogeosciences, 12, 2655-
1328 2694, 2015.
1329 Williams, A.P., Allen, C.D., Macalady, A.K., Griffin, D., Woodhouse, C.A., Meko, D.M. et al.:
1330 Temperature as a potent driver of regional forest drought stress and tree mortality, Nature
1331 Climate Change, 3, 292, 2012.
1332 Williams, A.P., Seager, R., Berkelhammer, M., Macalady, A.K., Crimmins, M.A., Swetnam,
1333 T.W. et al.: Causes and Implications of Extreme Atmospheric Moisture Demand during the
1334 Record-Breaking 2011 Wildfire Season in the Southwestern United States, J. Applied
1335 Meteorology and Climatology, 53, 2671-2684, 2014.
1336 Williams, L.J., Bunyavejchewin, S. & Baker, P.J.: Deciduousness in a seasonal tropical forest in
1337 western Thailand: interannual and intraspecific variation in timing, duration and
1338 environmental cues, Oecologia, 155, 571-582, 2008.

Wullschleger, S.D., Hanson, P.J. & Todd, D.E.: Transpiration from a multi-species deciduous forest as estimated by xylem sap flow techniques, For. Ecol. and Manage., 143, 205-213, 2001.

Xu, X., Medvigy, D., Powers, J.S., Becknell, J.M. & Guan, K.: Diversity in plant hydraulic traits explains seasonal and inter-annual variations of vegetation dynamics in seasonally dry tropical forests, New Phytol., 212, 80-95, 2016.

Yang, Y., Hillebrand, H., Lagisz, M., Cleasby, I., & Nakagawa, S.: Low statistical power and overestimated anthropogenic impacts, exacerbated by publication bias, dominate field studies in global change biology. Glob. Change Biol., 28, 969– 989, https://doi.org/10.1111/gcb.15972, 2022.

Zhu, K., Chiariello, N.R., Tobeck, T., Fukami, T. & Field, C.B.: Nonlinear, interacting responses to climate limit grassland production under global change, PNAS, 113, 10589-10594, 2016.

Zhu, Q., Riley, W.J., Tang, J., Collier, N., Hoffman, F.M., Yang, X. et al.: Representing Nitrogen, Phosphorus, and Carbon Interactions in the E3SM Land Model: Development and Global Benchmarking, 11, 2238-2258, 2019.

Zscheischler, J., Mahecha, M.D., von Buttlar, J., Harmeling, S., Jung, M., Rammig, A. et al.: A few extreme events dominate global interannual variability in gross primary production, Environ. Res. Lett., 9, 035001, 2014.